Environmental Science and Pollution Research (2022) 29:80137–80160
https://doi.org/10.1007/s11356-022-23407-9

REVIEW ARTICLE

Current and potential approaches on assessing airflow and particle dispersion in healthcare facilities: a systematic review

Huiyi Tan[1] · Keng Yinn Wong[2] · Mohd Hafiz Dzarfan Othman[3] · Hong Yee Kek[2] · Roswanira Abdul Wahab[3,4] · Garry Kuan Pei Ern[5,6] · Wen Tong Chong[7] · Kee Quen Lee[8]

Received: 18 May 2022 / Accepted: 27 September 2022 / Published online: 4 October 2022
© The Author(s), under exclusive licence to Springer-Verlag GmbH Germany, part of Springer Nature 2022

Abstract

An indoor environment in a hospital building requires a high indoor air quality (IAQ) to overcome patients' risks of getting wound infections without interrupting the recovery process. However, several problems arose in obtaining a satisfactory IAQ, such as poor ventilation design strategies, insufficient air exchange, improper medical equipment placement and high door opening frequency. This paper presents an overview of various methods used for assessing the IAQ in hospital facilities, especially in an operating room, isolation room, anteroom, postoperative room, inpatient room and dentistry room. This review shows that both experimental and numerical methods demonstrated their advantages in the IAQ assessment. It was revealed that both airflow and particle tracking models could result in different particle dispersion predictions. The model selection should depend on the compatibility of the simulated result with the experimental measurement data. The primary and secondary forces affecting the characteristics of particle dispersion were also discussed in detail. The main contributing forces to the trajectory characteristics of a particle could be attributed to the gravitational force and drag force regardless of particle size. Meanwhile, the additional forces could be considered when there involves temperature gradient, intense light source, submicron particle, etc. The particle size concerned in a healthcare facility should be less than 20 μm as this particle size range showed a closer relationship with the virus load and a higher tendency to remain airborne. Also, further research opportunities that reflect a more realistic approach and improvement in the current assessment approach were proposed.

Keywords Airflow distribution · Particle dispersion · Healthcare facilities · Numerical simulation · Onsite investigation · Healthcare-associated infection

Introduction

Indoor air quality (IAQ) is highly related to the pollutants which usually originate from the interactions of biological or chemical substances with indoor environments. A high level of contaminants could bring deteriorating impacts on the occupants' health (Chen et al. 2016; Villafruela et al. 2013). Understanding and controlling the level of indoor pollutants could minimize the risk of contracting relevant health issues. In general, there are various sources of indoor air contaminants, including outdoor air pollutants, building and furnishing materials and occupants' activities such as

Responsible Editor: Philippe Garrigues

✉ Keng Yinn Wong
kengyinnwong@utm.my

[1] School of Chemical and Energy Engineering, Faculty of Engineering, Universiti Teknologi Malaysia, Johor, Malaysia

[2] School of Mechanical Engineering, Faculty of Engineering, Universiti Teknologi Malaysia, Johor, Malaysia

[3] Advanced Membrane Technology Research Centre (AMTEC), Universiti Teknologi Malaysia, Johor, Malaysia

[4] Department of Chemistry, Faculty of Sciences, Universiti Teknologi Malaysia, Johor, Malaysia

[5] School of Health Science, Universiti Sains Malaysia, Kelantan, Malaysia

[6] Department of Life Sciences, Brunel University, Uxbridge, London, UK

[7] Department of Mechanical Engineering, Faculty of Engineering, University of Malaya, Kuala Lumpur, Malaysia

[8] Malaysia-Japan International Institute of Technology, Universiti Teknologi Malaysia Kuala Lumpur, 54100 Kuala Lumpur, Malaysia

cleaning, cooking, smoking, etc. (Vardoulakis et al. 2020). The IAQ could worsen when the ventilation rate is low and unable to remove these pollutants efficiently (Zhong et al. 2019). Therefore, proper assessments should be conducted to assess and maintain a desirable level of IAQ to protect the population's health (Vardoulakis et al. 2020).

Typically, a general hospital provides healthcare facilities ranging from small clinics to critical care centres such as operating rooms, extensive emergency rooms and trauma centres for patient treatment (ASHRAE 2019). These amenities require a healthy and pleasant environment for patients' recovery and efficient performance of medical staff (Bivolarova et al. 2016). Therefore, the IAQ in these facilities is more crucial than in other indoor environments. Due to the primary function of a hospital is centred on patient care (Nimlyat and Kandar 2015; Ryan-Fogarty et al. 2016), a proper and detailed method for evaluating the amount of contaminants in this environment should never be overlooked (Wong et al. 2019a).

The IAQ in healthcare facilities has been recognised as the main contribution to healthcare-associated infections (HAIs). HAI, also known as a nosocomial infection, is an infection acquired in a healthcare facility. It can spread to susceptible patients through various means, i.e. contact with infectious individuals, contaminated surfaces and exposure to exhaled droplets (Saw et al. 2021). HAIs significantly impact public health and the economy in terms of prolonged hospital stay, long-term disability, high treatment costs and excess death rates (Chen et al. 2016; Villafruela et al. 2013). According to a report, HAIs have increased the additional annual treatment cost by € 7 billion and $ 6.5 billion in Europe and the USA, respectively (Chen et al. 2016). The financial burden for HAIs treatment is expected to be higher in developing countries (Allegranzi et al. 2011). Villafruela et al. (2013) stated that HAIs caused 14.6% of death cases among hospitalised patients, whereas lower respiratory tract and surgical wound infections contributed 39% and 14% of total HAI reported cases, respectively.

Among the strategies adopted for reducing patients getting HAI, environmental infection control and engineering controls were proven to be effective (Prevention 2017). Environmental infection control includes the prevention of contamination and colonisation as well as direct infection. For instance, the mitigation measures such as social distancing, quarantine and isolation for the infectious individuals are among the primary barriers to combat cross infection through contact transmission. However, this preventative measure could not be applicable to those asymptomatic individuals with similar viral loads (Layden et al. 2020). On the other hand, engineering controls eliminate or reduce exposure to a chemical or physical hazard through the use or substitution of engineered machinery or equipment. They consist of ventilation rate, determination of airflow distribution, the layout of supply and exhaust air terminal devices, heat load distribution, room pressurisation, etc. (Bivolarova et al. 2016). Numerous studies have been conducted regarding engineering control, encompassing the optimal ventilation systems, high-performance filtration systems and dedicated air diffuser equipment (Liang et al. 2020; Sadrizadeh et al. 2021; Srivastava et al. 2021).

The ventilation rate in an indoor environment is measured based on its air change per hour (ACH) value. It is a quantity of the air volume added to or removed from a confined space divided by the volume of the space. A proper amount of air change rate can maintain the IAQ and overcome the risk of airborne cross-infection (Bivolarova et al. 2016). ASHRAE standard for ventilation of health care facilities (ASHRAE 2013) prescribed the ACH values for general patient rooms and infectious wards should fall within 4/h to 6/h and 12/h, respectively. Many studies have ascertained that the ACH significantly affects the quantity of contaminants in healthcare facilities (Faulkner et al. 2015; Hang et al. 2014; Li et al. 2014).

The use of a dedicated airflow ventilation system could also promote healthy IAQ. In general, vertical downward and horizontal supply air diffusers are commonly used inside a surgical room (Nastase et al. 2016; Olmsted 2008; Sadrizadeh and Holmberg 2014). Based on past reports, the unidirectional vertical airflow system was found to be more efficient for reducing the level of bacteria-carrying particles in a surgical area (Nastase et al. 2016; Sadrizadeh and Holmberg 2014). However, the horizontal airflow diffuser could usually cause deflection to the airflow and particle movement if a surgical staff is in the path of the flow. Aside from ventilation strategies, the amount of the contaminant could be managed by controlling the particle sources released rate through body exhaust suits and helmet systems (Sanzen et al. 1989; Wendlandt et al. 2016; Young et al. 2016).

The majority of review papers reflected on the disease control-related issues such as the effectiveness of ventilation strategies (Cao et al. 2014; Chow and Yang 2004; Yau et al. 2011), antimicrobial surfaces for lessening the HAIs (Muller et al. 2016), possible factors of transmitting the influenza virus (Otter et al. 2016) and risks of disease transmission associated with aerosol-generating medical procedures (Davies et al. 2009). However, the methods of assessing the IAQ in healthcare facilities have not been reported. The aim of this paper is to outline the methods used by previous studies in examining the IAQ in healthcare premises. The article begins with descriptions of field test procedures, followed by reporting on the numerical approach, summary and opportunity for future research.

Current assessment of airflow and particle concentration in healthcare facilities

Exposures to poor IAQ can result in unfavourable outcomes for patients and cause illness to medical staff. Therefore, several methods, including field test measurements, laboratory works

and numerical simulations, have been widely used to assess the IAQ in healthcare premises. Each method has its advantages and limitations, as addressed in the following sections.

Assessment using experimental setup/onsite measurement

A comprehensive understanding of the transmission of airborne bacteria in healthcare environments is best to be realised by observing the in-situ profiles through field test sampling since it represents the actual phenomena. However, evaluating the transmission of airborne bacteria has posed a challenge to researchers for more than a century (Haig et al. 2016). The standard field test approaches are microorganisms and air samplings. Though the fact that microorganism sampling is time-consuming, requires well-trained personnel and the results are not instantaneous, interest has grown in developing a correlation between microbiological and particle contaminants (Haig et al. 2016). Extensive studies have also been made to associate the particle sizes with the microorganisms. A recent study conducted in an ISO Class 7 operating room reported that there is a positive correlation between microbes and particulate matter 5 (PM 5) and particulate matter 10 (PM 10) of 7% and 15%, respectively (Tan et al. 2022c). Figure 1 shows the onsite sampling of particulate matter, microbial and airflow volume and room pressure difference that was conducted in healthcare facilities.

Throughout biological aerosol (bioaerosol) sampling approach, *Staphylococcus aureus* (S. aureus), *Pseudomonas aeruginosa*, *Acinetobacter baumannii*, *Klebsiella pneumoniae*, *Escherichia coli*, *Coagulase-negative Staphylococci* (CoNS), Methicillin-resistance *Staphylococcus aureus* (MRSA) are the main bacterial species found in the hospital indoor environment (Cabo Verde et al. 2015; Chen et al. 2016; Sadrizadeh et al. 2016a). Bioaerosol is a suspension of airborne particles that contain living organisms with a size range of 1 to 100 µm. Among those bacteria, MRSA is identified as one of the bacteria that showed increased resistance to conventional drugs. The following studies claimed that the *S. aureus* infection due to MRSA bacteria has risen by at least 68% (Chen and Huang 2014; Prevention 2007). According to the reports, the percentage of this type of infection is progressing from 2% (Sadrizadeh et al. 2016a), 22% (Sadrizadeh et al. 2016a), 64%(Weber et al. 2009), 70% (Blomquist 2006) to > 70% (Chen and Huang 2014) in the year of 1974, 1995, 2004, 2006, and 2010s, respectively.

In 2013, D'Alessandro et al. (2013) investigated the ability of dusting cloth pad (DC pad) to detect contamination of filamentous fungi in operating rooms. They claimed that the DC pad

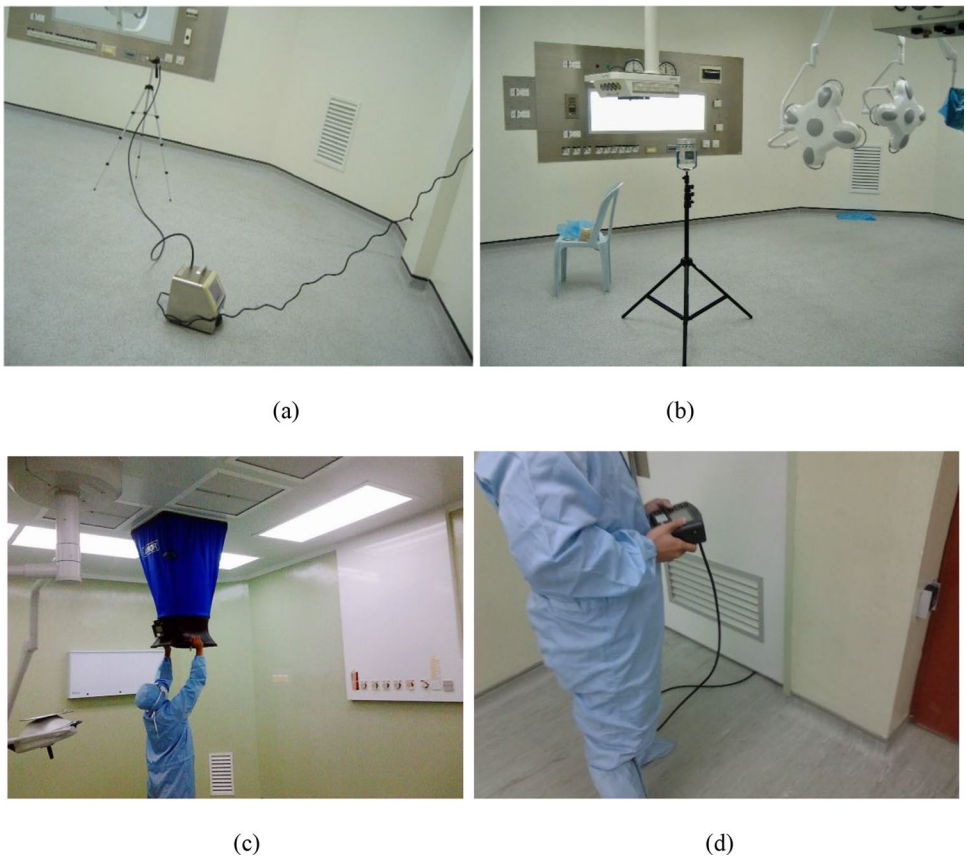

Fig. 1 Onsite sampling of **a** particulate matter (Tan et al. 2022c), **b** microbial counts (Tan et al. 2022c), **c** airflow volume (Kamar et al. 2020) and **d** room pressure difference (Kamar et al. 2020)

method is capable of determining environmental contamination and is a more sensitive approach than other surface samplings. Another biological sampling method used to correlate the frequently touched surfaces and the level of contamination in an operating room was conducted by (Link et al. 2016). Link's team discovered that the profound contact areas are highly contaminated, except for the frequently touched surgical table. In 2015, Saito et al. (2015) further (Link et al. 2016) studied by conducting a time-dependent approach, using both adenosine triphosphate (ATP) test and bacterial culture. Saito et al. (2015) encountered similar findings, and they further concluded that the ATP test could be utilised as a stable trace of contamination on environmental surfaces. However, the ATP test is not suitable to be used as an indicator for the number of viable microbes, as it is time-dependent and will decline over time.

With the ongoing COVID-19 pandemic spreading rapidly worldwide, researchers conducted the experimental investigations in the hospital areas to identify the potential presence of the SARS-CoV-2 virus to derive more specific prevention measures. Generally, literature reported two common sampling methods to detect the presence of SARS-CoV-2 virus: air sampling and surface swab sampling. For the surface swab method, the common practice is using a sterile swab previously soaked with virus transport medium (VTM) to move back and forth at the sampling area (Horve et al. 2021). Next, the swabbed sample was placed inside a tube containing VTM and stored carefully during the transport to the laboratory for further quantitative reverse-transcription polymerase chain reaction (qRT-PCR) testing (Horve et al. 2021). Meanwhile, the air samples collected at an ionization device using a collector plate with a low current of 80 μA and washed with VTM were demonstrated in the research work of Krambrich et al. (2021). Another approach to conducting air sampling is using a wetted wall cyclone sampler with a specific sampling flow rate (Guo et al. 2020).

The studies on the droplets of exhaled and coughed were experimentally investigated (Chao et al. 2009; Milton et al. 2013; Xu et al. 2017; Zhang et al. 2015). Milton et al. (2013) focused on the effectiveness of surgical masks in controlling the infectious droplets. Chao et al. (2009) examined the droplet size of coughing and speaking by employing the interferometric Mie imaging (IMI) technique. The IMI technique could quantify the droplets in proximity to the mouth and prevent the air sampling losses (Chao et al. 2009). Xu et al. (2017) also utilised the imaging method to explore the characteristics of exhaled airflow for predicting disease transmission. They found that the infectious risk depends on the breathing patterns and spatial distribution. The droplet characteristics, such as droplet size between gender, human health, and age, were revealed by Zhang et al. (2015). However, the droplet size variation was found to be insignificant across these parameters. Table 1 summarised the experimental approaches for quantifying the contamination in healthcare facilities.

Assessment using simulation approach in healthcare facilities

The fast growth of computational power has attracted the interest of many researchers in employing the numerical analysis. In addition, there are various benefits such as reliable results, shorter turnover time, lower cost and relatively straightforward to be carried out. Therefore, numerical studies have become the complementary approach to assessing the fluid–solid interaction in a confined space, such as healthcare facilities (Hang et al. 2015, 2014; Sadrizadeh et al. 2016b; Verma et al. 2017; Villafruela et al. 2013, 2019; Zhou et al. 2018), aircraft cabin (Chen et al. 2013; Duan et al. 2015; Li et al. 2016b; Lin et al. 2006; Poussou et al. 2010; Rai et al. 2014; Yan et al. 2016a; You et al. 2017, 2016a, 2016b), high-speed rail and bus cabins (Li et al. 2015a; Zhang and Li 2012; Zhu et al. 2012). One of the numerical analysis packages, computational fluid dynamic (CFD), has been widely used to analyse the interaction of airflow and particle transport in healthcare facilities. In general, CFD is a branch of fluid mechanics that employs numerical analysis and algorithms to solve and analyse problems that involve fluid flows. CFD provides a qualitative and quantitative prediction of fluid flows using mathematical modelling (partial differential equations), numerical methods (discretization and solution techniques) and software tools (solvers, pre- and post-processing utilities) (Aubin et al. 2004; Azmir et al. 2018; Cornelissen et al. 2007; Hong et al. 2017). Most of the CFD software are based on the solution of Navier–Stokes equations, the energy equation, the mass and concentration equations and the transport equations. There are two main types of techniques used in solving the Navier–Stokes equation, i.e. the finite element method (FEM) and the finite volume method (FVM). In recently reported literature, most researchers employed the FVM to solve the airflow and particle interaction in the indoor environment.

The numerical simulation method consists of several standard procedures such as domain modelling, field meshing, selections of airflow and particle tracking models, prescription of boundary conditions and analytical solutions. The descriptions of these methods have been discussed by many, among them are Romano et al. (2015) and Wang and Chow (2015). Usually, the computational domains are produced based on the actual dimension of the selected healthcare facilities. Sadrizadeh et al. (2014b) adopted a newly designed operating room in Sweden for contaminants investigation purposes. Yau and Ding (2014) opted for a heart surgery operating room situated in Malaysia. Meanwhile, Hang et al. (2014), Balocco and Lio (2011), Kim and Augenbroe (2013), and Adamu et al. (2012) selected six-bed, two-bed, single-bed isolation rooms and single-bed wards, respectively. They are authorised by several hospitals in Hong Kong, Italy, the USA and the UK. To reduce

Table 1 Summary of experimental studies on particle/microbial contamination for healthcare facilities

Authors	Experimental methods	Findings
Tan et al. (2022c)	Method: Biological surface sampling Sampling media: Tryptic Soy Agar (TSA) and Saboraud Dextrose Agar (SDA) Incubation: 35 °C for 2 days (for TSA); 30 °C for 10 days (for SDA)	Microbial counts have an evident correlation of 7% and 15% with particulate matter 5 (PM 5) and particulate matter 10 (PM10), respectively
Link et al. (2016)	Method: Biological surface sampling Sampling media: RODAC plates and cotton with buffered peptone water broth Incubation: 35 °C for 3 days	Among the high touch surfaces; i.e. anaesthesia computer mouse, surgical table, nurse computer mouse, operating room's door, and anaesthesia medical cart are highly contaminated except the surgical table
Saito et al. (2015)	Method: Biological surface samplings Sampling media: 1)ATP test: Monitoring system (Clean-Trace Hygiene Monitoring System) and luminometer (Clean-Trace Luminometer UNG3) 2)Microbial assessment: Culture plate (Petrifilm aerobic count plates) and 0.9% sterile saline Incubation: 32 °C for 48 h (For microbial assessment)	Adenosine triphosphate (ATP) results were strongly affected by the frequency of touching and orientation of environmental surfaces. The microbial counts declined over time, whereas the ATP results remain at a high level
Lewis et al. (2015)	Method: Biological surface samplings Sampling media: 1)ATP test: Getinge Safestep handheld luminometer and Safestep test swabs 2)Microbial assessment: RODAC plates Sample analysing: Within 60 s of collection (ATP test) Incubation: 35 °C for 24–48 h (Microbial assessment)	A single application of Isopropyl Organofunctional Silane (IOS) solution provides a persistent disinfectant activity, minimising microbial surface contamination in an environment where terminal cleaning may be inadequate or have limited effectiveness
King et al. (2013)	Method: Biological surface sampling Sampling media: Tryptone soya agar plates Incubation: 37 °C for 24 h	The transmission and settlement of small particles (pathogenic microorganisms) on surfaces are independent of the distance from the particle source
Barbadoro et al. (2016)	Method: Biological surface Sampling media: RODAC plates	Under real operational conditions, the bacterial contamination is higher in the turbulent air-supply operating room than the unidirectional air-supply operating room
Hang et al. (2015)	Method: Air sampling Sampling media: Multipoint sampler and doser- Type 1302 & 1303	Decreasing the duration of the door opening, raising air change rate or using an air curtain at the doorway are capable of reducing the particle contamination
Mousavi and Grosskopf (2015)	Method: Air sampling Sampling media: NUCON F-1000-DD forward light scattering photometric aerosol detector Time: 30-s intervals for a total of 30 min each	Aerosols with the size of less than 3 μm (viruses and most airborne bacteria) were found to be capable of migrating 9.5 m from a patient room to the nursing station in less than 14 min under directional airflow ventilation system
Hubad and Lapanje (2012)	Method: Active air sampling and biological sampling Sampling media: Filter system composed of a vacuum pump and flow controller at 11.5 L/min of airflow (Air sampling); SmartHelix Complex Samples DNA Extraction Kit (Biological sampling)	The ventilation system as recommended in the CDC guidelines effectively reduces the concentration of airborne Mycobacterium tuberculosis. The corridors and incubation room are the most hazardous areas in which healthcare workers can acquire the infection during working hours
Lapid-Gortzak et al. (2016)	Method: Air sampling Sampling media: Lighthouse 3016 particle counter Time: 30-s intervals	The used of unidirectional airflow (UDF) screen reduced the mean particle concentration (Particle size larger than 0.3 μm) on the instrument table by a maximum protection factor of 5
Månsson et al. (2015)	Method: Air sampling and biological sampling Sampling media: Sartorius MD-8 air scanner with a flow rate of 6 m^3/h (Air sampling); Blood agar plate (Biological sampling) Incubation: 35 ºC for 2 days	The nosocomial strains of *Staphylococcus* epidermis associated with prosthetic joint infections are not present in the unidirectional airflow supply during the prosthetic joint surgery

Table 1 (continued)

Authors	Experimental methods	Findings
Swan et al. (2016)	Method: Microbial sampling Sampling media: Cotton wool swabs, sodium thiosulphate (0.5%) solution, Columbia blood agar (CBA), R2A agar, P. Aeruginosa Selective (PAS) agar, sodium nalidixate and Pseudomonas (PA) agar Incubation: 30 °C for 48 h (PAS & PA); 37 °C for 48 h (CBA); 20 °C for 10 days (R2A)	The average bacteria density from untreated U-bends washbasin was more than 1×10^5 CFU/swab on all media. Manual and automated electrochemically activated (ECA) solution capable of reducing the bacteria counts less than 100 CFU/swab
Dai et al. (2015)	Method: Air sampling and biological sampling Sampling media: BAC-6825 fluorescent particle counter (Air sampling); Anderson impactor air sampler with a flowrate of 28.3 L/min for 5 min followed by blood agar plate (Biological sampling)	The fluorescent particle counters can be used to precisely measure a variety of laboratory-generated biologic particles such as Bacteroidetes subtilis and Escherichia colibacteria). Also, a high correlation coefficient of 0.76 was found between the biologic particle and bacteria counts
Yin et al. (2011)	Method: Air sampling and gaseous sampling Sampling media: TSI 3321 particle sizer spectrometer (Air sampling); INNOVA 1312 photoacoustic multi-gas analyser (Gaseous sampling)	The contaminant concentrations in the inpatient room for the case with the patient sitting on the bed were lower than those for the patient supine on the bed under the displacement ventilation system. The SF_6 tracer gas and 3 µm particles released at a notable initial velocity for simulating a cough give similar contaminant distributions in the inpatient room
(Birgand et al. 2015)	Method: Air sampling and biological sampling Sampling media: PMS particle counter with a flow rate of 0.0283 m^3/min with 1-min interval (Air sampling); Air-test Omega impactor air sampler at a flow rate of 100 L/min for 5 min on trypticase soy agar (Biological sampling) Incubation: 30 °C for 4 days	A strong correlation between air particle counts (0.3 µm, 0.5 µm and 5 µm) and microbial contamination was found. Unidirectional airflow can decrease the microbial air contamination during the surgery process
Jurelionis et al. (2015)	Method: Air sampling Sampling media: Handheld 3016 optical particle counters Sampling resolution/ duration: 1 s/ 10 min	At a lower air change rates (Less than 3/h or 4/h), one-way mixing ventilation directed particles towards air exhaust diffusers more efficiently, while four-way mixing ventilation enabled more particles to remain airborne
D'Alessandro et al. (2013)	Method: Air sampling and biological surface sampling Sampling media: Active air sample, RODAC contact plates and dusting cloth pad	Dusting cloth pad samples performed better in the ability to detect environmental contamination of filamentous fungi as compared to Rodac plates and air sampling
Helmis et al. (2007)	Method: Air sampling Sampling media: Automated Horiba analysers (NO_x, SO_2); PEM 200 particle samplers (PM10, PM2.5); IAQRAE and ppbRAE air quality monitors (TVOCs, CO_2)	The concentrations of CO_2, TVOCs, and particulate matters are high during the occupied condition. The concentrations of NO_x and SO_2 are low and independent of occupants
Pankhurst et al. (2011)	Method: Air sampling and biological sampling Sampling media: Lighthouse 3013 particle counters with 28.3 L/min (Air sampling); Tryptic soy agar (Biological sampling) Incubation: 37 °C for 24 h	The presence of people within the operating room had the greatest impact on both airborne bacteria and particle counts
Booth et al. (2013)	Method: Air sampling Sampling media: TSI PortaCount Plus particle counter	A surgical mask could reduce exposure to aerosolized infectious influenza virus with an average reduction of sixfold, depending on the design of the mask
Cabo Verde et al. (2015)	Method: Microbiological air sampling Sampling media: MAS 100 air sampler with flowrate of 100 L/min; Petri dishes, Tryptic Soy Agar (TSA), Malt Extract Agar (MEA) supplemented with antibiotic chloramphenicol (0.05%) Incubation: 30 ± 1 °C for 7 days (TSA); 25 ± 1 °C for 7 days	Staphylococcus (51%) and Micrococcus (37%) were dominant among the bacterial genera identified in hospital sites. Concerning indoor fungal characterization, the prevalent genera were Penicillium (41%) and Aspergillus (24%)

Table 1 (continued)

Authors	Experimental methods	Findings
Milton et al. (2013)	Method: Air sampling and biological sampling Sampling media: G-II exhaled breath collection system, SKC BioSampler (Air sampling); Swab wetted with Dulbecco's phosphate buffered saline with calcium and magnesium, Applied Biosystems Prism 7300 detection system, LightCycler 480, 1 µg/ml of TPCK-trypsin (Biological sampling) Sampling duration: 30 min (Air sampling) Incubation: 37 °C for 72–96 h (Biological sampling)	The fine particle contained 8.8 fold (95% confidence interval 4.1 to 19) more viral copies than the coarse particles. The surgical masks reduced the viral copy numbers in the fine fraction by 2.8-fold (95% confidence interval 1.5 to 5.2) and in the coarse fraction by 25 gold (95% confidence interval 3.8 to 180)
Chao et al. (2009)	Method: Imaging system (Particle Image Velocimetry and Interferometric Mie imaging) Imaging media: CCD Camera, laser sheet optics, polariser, Nd: YAG laser (Same for both imaging techniques) Specifications: Laser (532 nm wavelength with pulse width 3–5 ns; CCD camera (dual frame with resolution 1376 × 1040 pixels and a maximum frame rate of 10/s)	The average expiration air velocity for coughing and speaking are 11.7 m/s and 3.9 m/s, respectively. The evaporation and condensation effects had a negligible impact on the droplets. Also, the geometric mean diameter of droplets from and speaking are 13.5 µm and 16.0 µm, respectively
Romano et al. (2017)	Method: Air sampling Sampling media: TSI Ultrafine Particle Counter with flowrate 0.1 L/min Sampling time: 5 s	A unidirectional downward airflow removed the airborne contaminant better than an upward displacement airflow. Larger airflow volume capable of evacuating the surgical smoke at the surgical area faster and more efficient
Noguchi et al. (2017)	Method: Air sampling Sampling media: KC-52 Laser Particle Counter	A large number of particles were released during unfolding the surgical gown, removal of surgical gloves, and placing arms through the sleeves of the gowns. Laminar airflow managed to reduce the incidence of bacterial contamination near the operating table
Shaw et al. (2018)	Method" Biological sampling Sampling media: MAS-100 Viable Impactor Air Sampler with a flowrate of 100 L/min for 10 min, trypticase soy agar Incubation: 48 h at 35 °C	The mean microbial colony counts are low under the well-controlled ventilation system, and the absence of the medical personnel. The number of personnel and activities critically influenced the microbe concentration in the operating room
Choi et al. (2017)	Method: Air sampling Sampling media: Centre 342 Temperature Humidity Recorder (temperature and relative humidity), MAS 100 Eco Microbial Air Sampler (airborne bacteria), and TSI 7545 Indoor Air Quality Meter (carbon monoxide and carbon dioxide) Sampling time: < 30 s	The surgical smoke nearby patient's abdominal cavities contained high concentrations of volatile organic compounds including benzene and toluene, which exceeded the inhalation health guidelines. The concentrations of carbon monoxide and carbon dioxide in the operating room are not notable
Guo et al. (2020)	Method: Air and surface swab sample Sampling media: SASS 2300 Wetted Wall Cyclone Sampler at 300 L/min for 30 min, quantitative real-time PCR	The rate of SARS-CoV-2 positivity was relatively high for the surface of the objects that were frequently touched by medical staff or patients, including computer mice, trash cans, sickbed handrails and doorknobs
Horve et al. (2021)	Method: Surface Swab Sampling Sampling media: Puritan PurFlock Ultra swabs (catalog #25–3606- U) premoistured with viral transport media (RMBIO, catalog #VTM- CHT), conical tubes (Cole- Parmer, catalog #UX- 06,336–89) Sampling time: 20 s	The presence of SARS-CoV-2 RNA was detected in approximately 25% of samples taken from ten different locations in multiple HVAC air handling unit
Krambrich et al. (2021)	Method: Air and swab sampling Sampling media: sterile nylon flocked swabs soaked in virus transport medium VTM, a collector plate with a low current of 80 µA	SARS-CoV-2 virus in the hospital environment subsides in two states; as infectious and as non-infectious

the turnover time, a certain degree of simplifications was made on a human manikin model and interior furnished in the computational domain. Figure 2 shows some simplified computational domains used in previous studies.

Various approaches were used to simplify the human manikin model and furnishings for analysing their effects on airflow velocity distribution and contaminant transport. Yan et al. (2016b) claimed that such simplification has a significant effect on the thermal airflow field prediction, especially in the vicinity of the manikin surfaces. A similar finding was reported by Li et al. (2015c). They further claimed that a simplified mannequin could increase the predictive error of contaminant transport in the computational domain. One of the weak manikin models is a rectangular shape model, as shown in Fig. 2e because such configuration could produce a swirling flow in the head and leg sections of the manikin. Although a complete human model as illustrated in Fig. 2b and c could give better predictions on the airflow and particle dispersions, several researchers are still using simple manikin models for indoor study (Mahyuddin et al. 2015). The simplification was adopted as the complex geometry requires extremely fine grids, consumes enormously long computational time and demands a great effort to create a good quality mesh. The simplistic approach, however, is more favourable since it was proven to give reasonable solutions for airflow and particle dispersion in healthcare facilities.

Grid independence study is a procedure for inspecting the errors during the implementation of CFD models. An appropriate grid number is essential for a quick, accurate and efficient multiphysics solution at the cost of minimum affordable computational power. The primary purpose of carrying out grid independence analysis is to ensure the numerical solutions remain insignificant changes with further incrementing the number of grids. Grid convergence analysis or grid refinement study is the first procedure to verify CFD models (Kwaśniewski 2013). It is a process to estimate discretization errors in the CFD simulations and to check that the solutions are within the asymptotic range of convergence. The errors could be considered any difference between the exact solution of the governing equations (asymptotic solution) and the discretized system (Pletcher et al. 2012). These errors accumulated from the numerical algorithms, the mesh style and quality used to discretize the equations and boundary conditions (Ferziger and Peric 2012). The most traditional method implemented to estimate

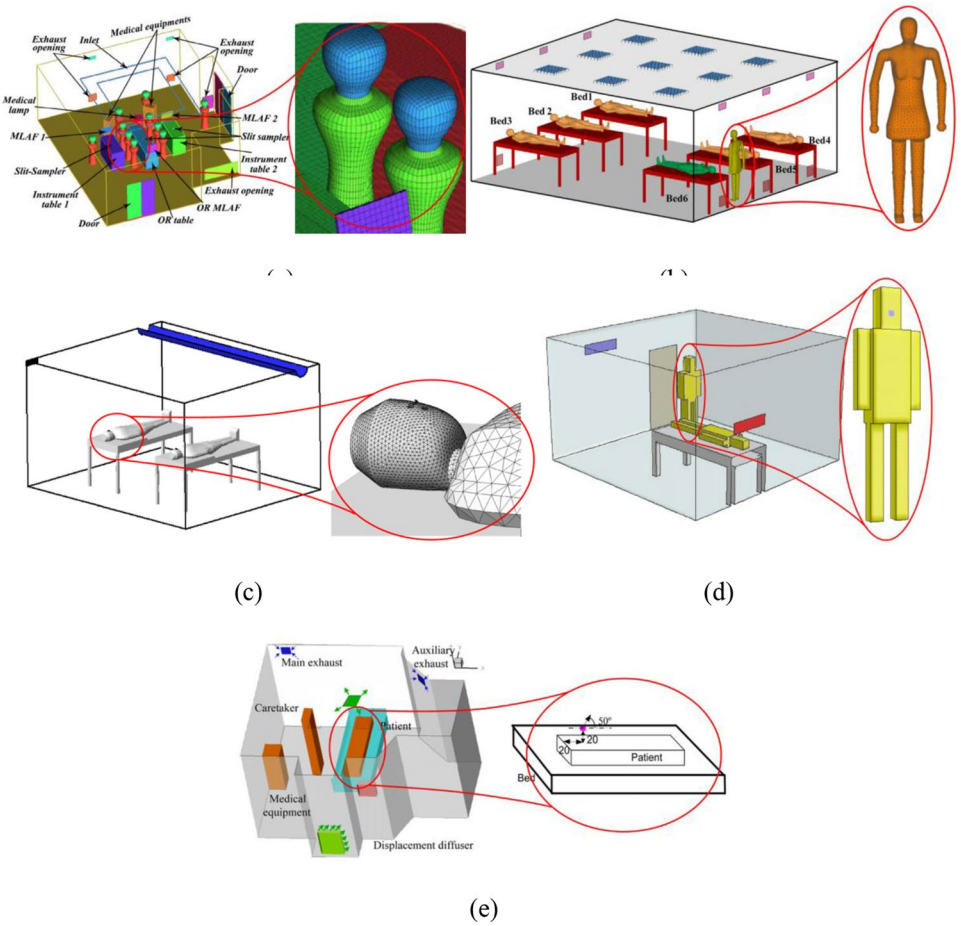

Fig. 2 Simplified human manikins and furnishings in **a** an operating room (Sadrizadeh and Holmberg 2015); **b** a six-bed isolation room (Hang et al. 2014); **c** a two-bed ward (Qian et al. 2008); **d** a single-bed isolation room (Shih et al. 2007); **e** a single-bed ward (Yin et al. 2011)

this error is Grid Convergence Index (GCI). The GCI is a relative error bound that describes the variation of solutions with mesh refinement. To ensure the solutions appear within the asymptotic range, the smaller the value of the GCI, the better performance of the predictions. The GCI is defined as (Karimi et al. 2012),

$$GCI_{fine} = \frac{F_s|\varepsilon|}{r^p - 1} \times 100 \tag{1}$$

In Eq. (2), F_s represents the safety factor, ε is the relative error, r is the grid refinement ratio and p is the formal order of accuracy of the algorithm (Karimi et al. 2012). Roache (1993) proposed using at least three grid refinements to maintain a constant reduction value. The r is determined to examine that only the discretization error is evaluated (Hurnik et al. 2015) and to meet the criteria, the value of r should be greater than 1.3. The r is described as the ratio of control volumes in the fine and coarse meshes, i.e.

$$r = \left(\frac{N_{fine}}{N_{course}}\right)^{\frac{1}{3}} \tag{2}$$

The values of ε and p are defined as the following,

$$\varepsilon = \frac{(f_2 - f_1)}{f_1} \tag{3}$$

$$p = \frac{\ln\left((f_3 - f_2)/(f_2 - f_1)\right)}{\ln(r)} \tag{4}$$

In the above equations, f_1 denotes the fine grid solution, f_2 is the medium grid solution and f_3 is the coarse grid solution. Roache (1993) suggested that the safety factor, F_s, should stay within the range of 1.25 (for three or more meshes) to 3 (for two meshes). A higher value of F_s represents a more stable level of confidence in the CFD solutions (Karimi et al. 2012). The F_s values were set based on the accumulated experience on the CFD calculations (Roache 1998). In the works done by Gilkeson et al. (2014), Sadrizadeh et al. (2016b) and Toja-Silva et al. (2015), they concluded that the grids are adequately fine when the GCI values are less than 3.4%, 6.1% and 5.77%, respectively. Salim et al. (2006) resolved that the satisfactory GCI value should not exceed 11.7% to achieve reasonable particle dispersion solutions. The GCI value decreases for the successive grid refinements, indicating the dependency of the numerical simulation on the element size has been reduced. Significant reduction of the GCI from the coarser grid to the finer grid shows that the grid-independent solution has nearly been achieved. Further grid refinement will yield an insignificant change in the simulation results. According to Volk et al. (2017), the GCI value of less than 10% could be considered acceptable.

Airflow models

Some previous works have used a smoke technique (Calautit and Hughes 2014; Wagner and Schreiber 2014; Yin et al. 2016) or particle image velocimeter (PIV) method (Fu et al. 2016; Li et al. 2016a, 2015b; Reyes et al. 2015) to visualize the airflow. However, due to the enormous investment cost needed to conduct a PIV experiment in a full-scale chamber, this approach is rarely used (Huang et al. 2021). Moreover, a smoke visualization technique was designed to supplement the PIV measurement and claimed to be most suited for small-scale studies for visualising the flow structures (Tao et al. 2018). In contrast, a numerical method has been widely utilised for a similar purpose, to predict and visualise the airflow pattern in healthcare buildings with the explosively growing computational power (Nielsen 2015). Generally, the process includes prescribing the exact values at the domain boundary, discretizing the domain into finer elements, choosing the appropriate flow model, and calculating the solution. A suitable airflow model is essential to describe the airflow phase and to obtain reasonable solutions. This could only be accomplished through comprehensive verification and validation of some selected flow models.

To predict particle dispersion inside a domain, the classification of fluid flows is necessary. One of the essential flow characteristics that must be considered in the CFD analysis is the type of fluid phase, either a single-phase or two-phase flow. For tracking the interface of two distinct phases, i.e. air (fluid) and solid (particle), which are not interpenetrating, the two-phase flow option is always activated. The airflow phase is treated as the primary phase, simulated in a continuous scheme using a suitable flow model. Next, the particle phase is prescribed as the second phase, dispersing within the continuous phase. The particle is simulated via an appropriate particle model in a discrete manner.

As air is the primary carrier of heat and airborne contaminants in the healthcare facilities such as patient rooms, isolation rooms, anteroom and operating rooms, the direction of the airflow becomes one of the concerned parameters to be examined. Some scholars have perceived that a unidirectional airflow could reduce the surface contaminant and enhance the airborne particle removal efficiency. An inversely proportional relationship between the displacement rate of particles and the number of escaped particles was discovered. Also, there are studies on the locations of supply air diffusers and returned outlets on the indoor particle distribution. One of the cases was a study done in a patient room by Khankari (2016) to investigate the possible flow path of airborne pathogens and thermal comfort on occupants. During the past outbreaks of Severe Acute Respiratory Syndrome (SARS), Influenza and Ebola diseases, studies concerning ventilation systems in isolation rooms were carried out by several researchers. The sources

of airborne particles are always suspected from the outside air. The isolation building was conventionally created to control epidemics from spreading. Due to its provision, it must remain closed continually. To test the hypothesis, Park and Sung (2015) selected a patient ward to determine the amount of leakage air through tracer gas tests and CFD methods. Chow et al. (2006) numerically assessed the effects of the pressure differential between the inside and outside of an operating room on the airflow characteristics. Table 2 summarised the configurations used to simulate the airflow in healthcare facilities.

Based on the literature listed above, almost all the airflow studies in healthcare buildings applied the wall treatment. In general, the wall treatment function could increase the reliability of predicting airflow in the region near the wall. In contrast, the absence of wall treatment could over predict the turbulent kinetic energy which acts normal to the wall. To the authors' knowledge, standard wall functions and enhanced wall treatment are the most favourable choices for the wall treatment. However, employing the enhanced wall treatment when choosing the k-ε and k-ω models is highly recommended to solve the airflow. It provides the most consistent wall shear stress and wall heat transfer predictions with the least sensitivity to y^+ value (Fluent 2009). If wall functions are enabled, grids with a fine near wall spacing should be avoided, and y^+ value of more than 30 is recommended (Fluent 2009). As far as concerned, the wall functions do not provide a systematic refinement on the near wall grid. Also, it is not suitable for low to medium turbulent ($10^4 < \mathrm{Re} < 10^6$) flow analysis (Fluent 2009).

To achieve convergence and a stable solution, it is an excellent option to examine the residual levels and monitoring of the integrated quantities (Fluent 2009). In most cases, the residual criteria of 10^{-6} for the energy equation and 10^{-3} for other equations are sufficient (Fluent 2009). Villafruela et al. (2013) recommended 10^{-5} for continuity, momentum, energy and turbulence equations and 10^{-7} for contaminant concentration equations based on the particle contamination study in an isolation room. Gilkeson et al. (2014) proposed a tighter limit of 10^{-8} for the momentum equation to achieve better accuracy. Sadrizadeh and Holmberg (2015), however, claimed that the convergence criteria of 10^{-5} for continuity and energy equations are adequate in obtaining a converged solution. The complete verification procedures have been demonstrated by Peng et al. (2016), and they concluded that a slight difference in the convergence criterion of 10^{-3} and 10^{-5} could cause the simulation result to vary significantly (Peng et al. 2016). So far, there is no consensus on the convergence criterion for indoor analysis. In our view, a converged solution does not mean that the convergence criterion needs to achieve a huge drop in the residuals. Sometimes, when there is a great initial guess on the solution, it is almost impossible for the residuals to drop to three orders of magnitudes (Fluent 2009). Therefore, verification of the convergence criterion should be performed to obtain a converged solution.

Particle dispersion models

To ensure a highly conducive environment in the healthcare facilities, e.g. operating room, isolation room, intensive care unit (ICU), strict rules and procedures are implemented on the premises. Hoffman et al. (2002) discovered that majority of the airborne bacterial contamination in the operating room is released from the surgical personnel. The identified contaminant that causes the infection is the squames or skin scales (Chow and Wang 2012; Woods et al. 1986). These sources are detached from the body due to the friction actions of clothing and human movement. To encounter this issue, one of the procedures is to oblige the surgical team to be dressed in a cleanroom suit. This procedure could ensure a massive reduction in the amount of squames or skin scales from the personnel shedded to the environment. Figure 3 illustrates the skin scales under the scanning electron micrograph.

The skin scales are present in irregular shapes and dimensions. It is almost impossible to precisely model each squame for the purpose of simulation. Therefore, people tended to correlate the skin scale size with the aerodynamic particle size. The term bacteria-carrying particles (BCPs) has then been employed to represent the squames or skin scales, especially for the application in the indoor environment simulation. Sadrizadeh et al. (2016a) claimed that particles with a diameter of 4–60 µm could represent BCPs. They further concluded that those bacteria have an average diameter of 12 µm. Hansen et al. (2005) also revealed that skin scales are the main source of bacteria in the operating room. They ascertain that the BCPs fall within a narrow range, which is between 5 and 10 µm. A similar result was also discovered by Memarzadeh and Manning (2003), who scrutinised the ventilation system strategy to reduce the risk of surgery in an operating room. In contrast, Morawska et al. (2009) examined the droplet size of coughs, sneezes, talks or breaths prior to the simulation work in an isolation room. This research team noticed that most human exhaled droplets are in submicron ranges. Meanwhile, Chao et al. (2009) reported that the mean diameter of droplets for coughing and speaking are 13.5 µm and 16.0 µm, respectively. In a more recent study, Zhang et al. (2015) claimed that the droplet size study between healthy people and patients are 0.1–10 µm and 0.05–10 µm, respectively.

In the application of CFD, two main particle models are available for calculating the particle movement, namely Lagrangian particle tracking and Eulerian particle tracking. Both models predict the flow field based on the Eulerian framework, while the particle phases are treated according to

Table 2 An overview of the CFD airflow setups

Authors	Models/Setup configurations	Air supply	Wall treatment/y^+	Findings
Sadrizadeh et al. (2016b)	Model: RNG k-ε Discretise scheme: QUICK Algorithm: SIMPLE	Ceiling mounted inlet ~ Air flow rate: 2000 L/s; temperature: 20 °C; turbulent intensity: 5% Side wall outlet ~ Pressure: 10 Pa; turbulent intensity: 5%	Enhanced wall treatment; $y^+ \cong 2$; GCI values less than 6.1%	The simulated airflow by utilising the RNG k-ε model agreed well with the measurement result. The comparison was conducted at two different heights, namely 0.8 m and 1.2 m above floor level. At each height, air velocity magnitude for five coordinates was compared
King et al. (2013)	Models: RNG k-ε and RSM model Discretization scheme: Second order upwind scheme Algorithm: SIMPLE	High-level wall mounted inlet ~ Air change rate:6/h, temperature: 21.8 °C Low-level wall mounted outlet	Standard wall functions; $30 \leq y^+ \leq 300$	Reynolds Stress (RSM) turbulence model yield significantly better results than the RNG k-ε model
Hang et al. (2015)	Model: RNG k-ε Discretise scheme: Second order upwind scheme Algorithm: SIMPLE	Ceiling mounted inlet ~ Air flowrate: 0.066 m^3/s (66 L/s); velocity: 0.184 m/s, 0.486 m/s, and 1.21 m/s; temperature: 15 °C	Standard wall function; User-defined functions on the dynamic mesh	The results obtained from RNG k-ε model has a high correlation with the measured temperature and velocity distributions in isolation room and anteroom
Hang et al. (2014)	Model: RNG k-ε Discretise scheme: Second order upwind scheme Algorithm: SIMPLE	Ceiling mounted inlet: ~ Velocity: 0.12 m/s; temperature: 293.15 K Low-level wall mounted outlet ~ Outflow: Zero normal gradient	Standard wall function; No slip wall; User-defined functions on the dynamic mesh	The Large Eddy Simulation (LES) is not used as unsteady flow fields with human movement require very demanding computer memory and a long calculation time. The selection of the turbulence model is based on the recommendation from Zhang et al. (Zhang et al. 2009)
(Sadrizadeh et al. 2016a)	Model: Realisable k-ε Discrete scheme: QUICK Algorithm: SIMPLE	Ceiling mounted inlet ~ Air flow rate: 2000 L/s; temperature: 20 °C; room pressure: + 15 Pa, heat source: 116 W/m^2	Enhanced wall treatment; $y^+ \cong 2$; No slip conditions	Realisable k-ε is less demanding in terms of computational time than the RNG k-ε, which was derived to handle the swirl effect on turbulence
Chang et al. (2016)	Model: RNG k-ε Discrete scheme: Second order upwind scheme Algorithm: COUPLED	No inlet or outlet used in the domain. The author only focuses on the effects of door opening and closing	Near-wall treatment; User-defined functions on the dynamic mesh	Standard k-ε model is not reliable in predicting the regions with low velocities and thus low Reynolds numbers, particularly in the near wall regions. RNG k-ε model combined with appropriate treatment of the near-wall region gives a better prediction of indoor airflow
Villafruela et al. (2013)	Model: RNG k-ε Discrete scheme: Second order upwind scheme Algorithm: SIMPLE	Inlet ~ Air flow rate: 400 m^3/h	Standard wall functions; $30 < y+ < 60$	The simulated results validated well with the experimental data (Using the photoacoustic spectrometer measurement) conducted by Mendez et al. (Méndez et al. 2008)

Table 2 (continued)

Authors	Models/Setup configurations	Air supply	Wall treatment/y^+	Findings
Lee et al. (2016)	Model: High-Reynold-number k-ε Discrete scheme: Monotonic upstream-centred scheme for conservation law (MUSCL) Algorithm: SIMPLE	No inlet or outlet used in the domain. The author only focuses on the effects of door opening and closing $T_{indoor} = 20$ °C $T_{corridor} = -5, 0, 5, 10, 15$ °C (five cases)	Moving mesh to prescribe door movement. Information on wall function is not discussed	The standard k-ε turbulence model used in the CFD simulation uses the Reynolds average, so precise changes in turbulence characteristics over time could not be reproduced. However, the variations in the airflow characteristics were in good agreement with experimental data
Romano et al. (2015)	Model: Realisable k-ε Discrete scheme: Second order upwind scheme Algorithm: SIMPLE	Ceiling mounted inlet ~ Velocity: 0.25 m/s, 0.35 m/s, 0.45 m/s; turbulent intensity: 5% Low-level wall mounted outlet ~ Outlet: Zero gradient	Enhanced wall treatment; No slip conditions; $1 < y+ < 7$	The Realisable k-ε model shows a good agreement with experimental data (Mock setup includes dummies)
Yan et al. (2016b)	Model: RNG k-ε Discrete scheme: - Algorithm: SIMPLEC	–	Wall function is not discussed; $y^+ < 3$	The RNG k-ε model predicted well for the multiphase flows with the presence of human manikin and thermal conditions
Liu et al. (2015)	Model: Realisable k-ε Discrete scheme: Second order upwind scheme Algorithm: Not mention	Ceiling mounted inlet ~ Mass flow: 2.186 kg/s; temperature: 24.5 °C; relative humidity: 50%	Wall function is not discussed; No slip wall	The selection of airflow model is mainly based on the experimental and numerical findings of Kuznik et al. (2007)
Jin et al. (2016)	Model: RNG k-ε Discrete scheme: Second order upwind scheme Algorithm: SIMPLE	Inlet flow rate: 260 m^3/h, 520 m^3/h, and 970 m^3/h; Surface temperature: 398 K (Adiabatic)	Wall function	The isotropic assumption is not appropriate in near-wall areas where the turbulent kinetic energy normal to the wall is substantially smaller than the ones parallel to the wall
Yu et al. (2017)	Model: RNG k-ε Discrete scheme: Second order upwind scheme Algorithm: PISO	Ceiling mounted inlet ~ Mass flow rate: 1 24 kg/s; temperature: 285 K Walls, ceiling, floor and beds: Temperature: 295 K (adiabatic)	Standard wall function; No slip wall	For the indoor airflow simulations, RNG k-ε model was tested to be an appropriate choice as compared to other airflow models. Also, this model offered better accuracy and stability in cases of low Reynolds number and near-wall flows
Gilkeson et al. (2014)	Model: RSM Discrete scheme: Second order upwind scheme Algorithm: SIMPLER	Side window inlet ~ Velocity: 0.146 m/s, 0.438 m/s, and 0.876 m/s; turbulent intensity: 10% Sidewall outlet ~ Pressure: -5 Pa	Standard wall function; $15 \leq y^+ \leq 38$	The Reynolds Stress Model (RSM) yield a better prediction of bioaerosol dispersion in a mechanically ventilated room as compared to RANS models. The RMS model accounts for the anisotropic turbulent structures in contrast to RANS models
Tao et al. (2016)	Model: RNG k-ε Discrete scheme: QUICK Algorithm: SIMPLE	No inlet airflow. Human walking speeds are 0.4 m/s, 0.8 m/s, and 1.6 m/s	Wall function is not discussed (Authors focused on the dynamic mesh); $y^+ < 5$	The RNG k-ε showed a higher accuracy, computing efficiency and robustness as compared to SST model in predicting the airflow in indoor environments

Table 2 (continued)

Authors	Models/Setup configurations	Air supply	Wall treatment/y^+	Findings
Balocco et al. (2015)	Model: Standard k-ε Discrete scheme: -Second order upwind scheme	Ceiling mounted inlet ~ Velocity: 0.66 m/s, Turbulence intensity: 5%	Logarithmic wall functions	The simulated airflow results using standard k-ε model showed a good agreement with the previous literature (Al-Waked 2014; Ho et al. 2009)
Al-Waked (2014)	Model: k-ε Discrete scheme: - Algorithm: SIMPLEC	Ceiling mounted inlet ~ Velocity: 0.33 m/s, temperature: 20 °C	Wall function is not discussed	The k-ε model showed the most appropriate choice for investigating the airflow and particle dispersion in an operating room
Ufat et al. (2017)	Model: k-ε Discrete scheme: - Algorithm: SIMPLE	Ceiling mounted inlet ~ Velocity: 0.2 m/s, Turbulence intensity: 5% Hydraulic diameter: 3 m	Standard wall function;	The standard k- ε model demonstrated an acceptable simulation result as compared to the measurement data
Kamsah et al. (2018)	Model: RNG k-ε Discrete scheme: second order upwind scheme Algorithm: SIMPLE	Ceiling mounted inlet ~ Turbulence intensity: 20% Velocity: 0.32 m/s Temperature: 19 °C	Wall function is not discussed; No-slip wall	The RNG k-ε provides sufficient reliatble airflow results under a steady-state condition
Tan et al. (2022b)	Model: RNG k-ε Discrete scheme: second order upwind scheme Algorithm: SIMPLE	Ceiling mounted inlet ~ Turbulence intensity: 5% Velocity: 0.43 m/s Temperature: 19 °C Air curtain ~ Turbulence intensity: 10% Velocity: 0 m/s–1.2/s Temperature: 19 °C	Wall function not discussed; 5-inflation layers at all, with growth rate of 1.2; No-slip wall	The RNG k-ε model provides the best prediction of airflow in the ISO grade operating room, with a relative error of 9.62%. Standard k-ε, SST k-ω and standard k-ω models yielded a larger relative errors of 10.55%, 11.20% and 10.81%, respectively
Satheesan et al. (2020)	Model: Standard k-ε Discrete scheme: second-order upwind scheme Algorithm: SIMPLE	Ceiling mounted inlet ~ ACH: 6,9,13 temperature: 12 °C	Enhanced wall function; No-slip wall	The RNG k-ε model offers better accuracy, stability and computing efficiency for low reynolds number as well as near wall flows
Tan et al. (2022a)	Model: RNG k-ε Discrete scheme: second order upwind scheme Algorithm: SIMPLE	Ceiling mounted inlet ~ Turbulence intensity: 5% Velocity: 0.43 m/s Temperature: 19 °C Mobile air unit ~ Turbulence intensity: 5% Velocity: 0.1 m/s–0.6 m/s Temperature: 19 °C	Enhanced wall function; No-slip wall	The RNG k- ε model reflects a better airflow prediction in the ISO class cleanroom. The averaged relative error of RNG k-ε, relizable k-ε, and standard k-ε are 8.54%, 9.60% and 9.03%, respectively
Saw et al. (2021)	Model: Standard k-ε Discrete scheme: - Algorithm: -	Ceiling mounted inlet ~ Turbulence intensity: 5% temperature: 24 °C	Scalable wall function; No-slip wall; $y^+ \simeq 11$	The Standard k-ε model is proven suitable to simulate the flow conditions in the hospital ward

Table 2 (continued)

Authors	Models/Setup configurations	Air supply	Wall treatment/y^+	Findings
Wang et al. (2020)	Model: RNG k-ε Discrete scheme: Second-order upwind scheme Algorithm: SIMPLE	Air curtain inlet Velocity: 3.5 m/s	Standard wall function; No slip wall, $y^+ < 5$	The RNG k-ε turbulence model is widely utilised in the prediction of room air distribution as agreed by previous literature (Nielsen 2015)
Srivastava et al. (2021)	Model: RNG k-ε Discrete scheme: - Algorithm: SIMPLE	Ceiling mounted inlet ~ Velocity: 5.2 m/s temperature: 14.5 °C	Wall function is not discussed	The simulated results agreed well with the measured data from (Srebric and Chen 2002)
Lu et al. (2020)	Model: RNG k-ε Discrete scheme: - Algorithm: SIMPLE	Ceiling mounted inlet, Horizontal wall mounted inlet ~ ACH: 12 temperature: 22–24 °C	Standard wall function; Adiabatic wall	Excluding the experimental errors, the simulated results achieve a good consensus with the measurement data in the occupied zone

the particle tracking model selection. Zhang and Chen (2007) has demonstrated that these two models are well estimated the particle distribution in an aircraft cabin. So far, the use of the Eulerian particle tracking model in healthcare facilities has not been reported. The Lagrangian model is identified as the most favourable particle tracking model in the operating room, isolation room and patient wards. The two main reasons that the Lagrangian model is extensively adopted are (i) computational time is significantly reduced and (ii) the result is reliable when the particle volume is considerably lower than the fluid volume (less than 10–12%) (Romano et al. 2015). The approximation of the particle trajectory using the Lagrangian model could be expressed as Eq. (3):

$$\frac{du_p}{dt} = F_D\left(u - u_p\right) + \frac{g(\rho_p - \rho)}{\rho} + F_a \tag{5}$$

where u_p and u are the particle and air velocity vectors, respectively; F_D (u—u_p) is the drag force per unit of particle mass; ρ_p and ρ are particle and air density, respectively; g is the gravitational acceleration vector; and F_e is additional force per unit mass. Most of the researchers found an excellent agreement between the Lagrangian particle tracking model and the measured particle distribution in healthcare facilities. In 2015, Jin et al. (2015) validated the simulated particle concentration with the experimental data (Lu et al. 1996). A similar approach was performed by Sadrizadeh et al. (2016a) and Sadrizadeh and Holmberg (2015). They validated the Lagrangian model with the data published by Chen et al. (2006).

Activating the appropriate forces on the particle is significant in predicting particle trajectory behaviours. The common forces reported in the indoor building simulations include gravitational force, drag force, Brownian force, Saffman's lift force, thermophoretic force and pressure gradient force. The combination of gravitational, drag, Brownian and Saffman's life forces are claimed to be important in simulating the airflow and particle distribution in the healthcare premises (Mousavi and Grosskopf 2015). This finding is supported by Wang and Chow (2011), who simulated the fine particle movement in an isolation room. One year later, Chow and Wang (2012) revealed that the Brownian force is negligible towards the particle with a size larger than 0.01 μm. However, the gravitational and drag forces should not be disregarded in all particle sizes. For a non-isothermal study, the effect of thermophoretic force was found to produce a noticeable impact on the airflow and particle trajectory. Also, photophoresis force could be another interesting aspect, as most of the lights used in healthcare facilities were categorised as intense light. The summary of the forces applied to the particles in previous studies is tabulated in Table 3.

Based on the literature, the particle size ranges from 0.3 to 20 μm are widely treated as the BCPs or droplets

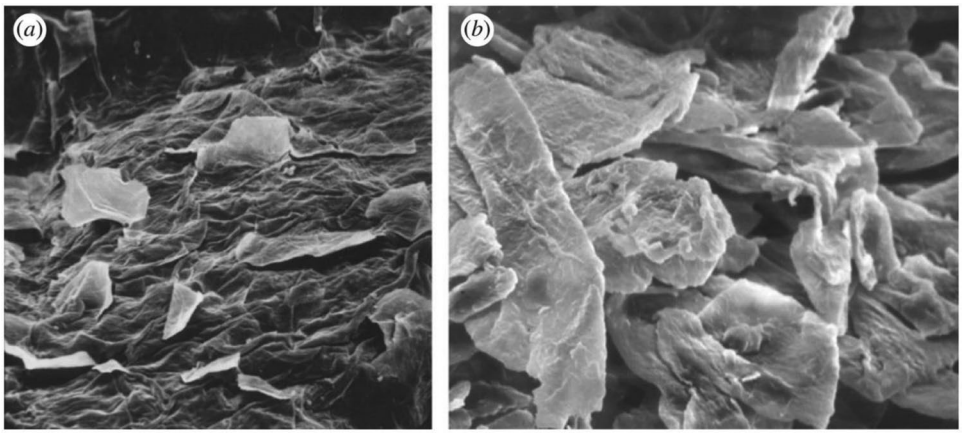

Fig. 3 Scanning electron micrograph of skin scales **a** nearly to be detached from the skin surfaces; **b** sampled from the air (Clark and de Calcina-Goff 2009)

that could pose a risk of healthcare-associated infections. However, a particle that is coarser in size (> 20 μm) can be disregarded in simulation as the potential of containing the virus is significantly lower than the finer particle (Milton et al. 2013). Also, such particles will rapidly settle onto the surface without being sustained in the air for a longer time (Wang and Chow 2011). Hence, the tendency of a coarse particle to spread as the airborne BCPs is reduced.

Opportunity to improve the reliability of the current assessment approach

In the past decade, the analysis of human presence in the healthcare premises is mainly conducted under a time-independent and unmoved condition. However, in an actual scenario, performing movements by the medical staff and objects are unavoidable. Therefore, recent research has focused on the dynamic approach rather than the static analysis as such approach reflects more realistic and reliable predictions of the IAQ in healthcare facilities (Kalliomäki et al. 2016; Tao et al. 2016). So far, only a few studies have examined the motion effects, i.e. door opening and closing, translational movement performed by medical staff, and upright to bending posture of the surgeon. The idea of assessing the effect of movement in the healthcare facility was first initiated by Tang et al. (2005) through an experimental study. They intended to prevent the infectious bacteria in the negative pressure isolation room from transmitting to the adjacent zones. Also, Shih et al. (2007) numerically followed up the moving action on the lateral walking motion performed by the medical staff in an isolation room. Afterwards, the numerical simulation approach on the dynamic movement has been discontinued till recently. The reasons are stated as follows; validating the simulated work is challenging as high-quality experimental data are rare (Hang et al. 2014), consuming a long turnaround time due to the fine mesh around the moving object (Fontanesi et al. 2015; Hang et al. 2014), handling the moving object is complicated due to the prescription of proper time-step size and particle tracking model (Wang and Chow 2015) and requiring intensive effort to write the specific-defined mathematical/ user-defined function (UDF) codes that designate the motions.

However, the assessment of the moving effects had been recommenced by Kalliomäki et al. (2016). Their research team experimentally investigated the impact of human movement on the airflow patterns and air volume exchange at the isolation room's doorway. Meanwhile, Tao et al. (2016) employed a numerical simulation method to analyse the human moving effects on the particle distribution. The airflow momentum induced by the moving body caused the 2.5 μm particle that was initially resting on the floor to lift and become re-suspended due to its interaction with the trailing wake. Amazingly, Mousavi and Grosskopf (2016) combined experimental and computation studies to assess the effects of the door opening in an isolation room. Moreover, the airflow was significantly disrupted by the door opening motion and the movement of objects. Based on the reported findings, it could be concluded that all the results obtained from a static condition vary from those results which considered the movement effects. In other words, it is necessary to consider the influences of movement in order to represent a realistic scenario in healthcare facilities.

Up to authors' knowledge, the studies on movement have been conducted by the experimental works, the numerical simulation or combination of both. In the experimental approach, Kalliomäki et al. (2015) controlled the movement sequences of human manikin by a computer program. The foamed plastic-made manikin was placed on a small cart with the mechanism of a motorised rail running embedded on the floor. Surprisingly, Wu and Lin (2015) employed real humans to investigate the influence of motion under three types of air distribution. Compared to Kalliomäki et al.

Table 3 A summary of the forces acted on various sizes of particle in healthcare facilities

Authors	Particles size	Forces	Findings
Sadrizadeh et al. (2016b)	12 µm in mean aerodynamic diameter	Drag force, gravitational force, Saffman's lift force	Effects of Saffman's lift force on the fine particles are relatively large, especially in the regions located near the operating room walls
Tao et al. (2016)	2.5 µm in diameter (Density: 700 kg/m^3)	Drag force, gravitational force, Saffman's lift force	The moving manikin causes a pronounced lifting effect on the micron-sized particles, which settle on the floor. The electrostatic and adhesion force at the particle–wall contact surface are disregarded
Sadrizadeh et al. (2016a)	12 µm in mean aerodynamic diameter	Drag force, gravitational force, Brownian force	A modified Discrete Random Walk model by implementing a damping function is required to improve the particle deposition prediction. An isotropic dissipation of the turbulence kinetic energy will cause an over-prediction of particle deposition
Wang and Chow (2015)	0.5 µm, 5 µm, 10 µm, and 20 µm (Density: 600 kg/m^3)	Gravitational force, Brownian force, Saffman's lift force, thermophoretic force	20 µm particles will settle rapidly onto surfaces while particles fall within the range of 0.5 µm and 20 µm suspended in the air for a longer time
Sadrizadeh and Holmberg (2015)	10 µm in diameter (Density: 1400 kg/m^3)	Drag force, gravitational force, Brownian force	Basset, pressure gradient and virtual mass forces are negligible compared to the drag force. Therefore, the variation in particle size had a negligible effect on particle trajectory, and those minor differences are due to the slightly different drag and gravitational forces acting on the particles
Sadrizadeh et al. (2014b)	5 µm, 10 µm and 20 µm in aerodynamic diameter	Drag force, gravitational force	Particle dispersion highly depends on Stokes number (STK). Particles with STK < 0.1 will follow airflow streamlines closely. A small STK value will cause insignificant trajectory differences between 5 µm and 20 µm particles
Sadrizadeh et al. (2014a)	10 µm in diameter (Density: 1400 kg/m^3)	Drag force, gravitational force, Saffman's lift force	The effects of pressure gradient, Basset, virtual mass, thermophoretic and Brownian forces are negligible as compared to drag force
Chow and Wang (2012)	5 µm, 6 µm, 8 µm, 10 µm in diameter (Density: 1000 kg/m^3)	Gravitational force, Brownian force	Effects of Brownian force on particle size larger than 0.01 µm are negligible
Wang et al. (2012)	0.3 µm in diameter (Density: 1050 kg/m^3)	Drag force, Saffman's lift force, Brownian force	Gravitational force is insignificant for particles with 0.3 µm in diameter as the particles have approximately the same diffusion properties as a gas
Wang and Chow (2011)	0.5 µm, 5 µm, 10 µm, 20 µm in diameter	Drag force, gravitational force, Brownian force, Saffman's lift force, thermophoretic force	Brownian and Saffman's lift forces are significant for the room airflow involving fine particles. The thermophoretic force due to temperature gradient was found to be critical in the case of nonisothermal airflow
Liu et al. (2009)	5 µm, 7 µm, 10 µm in diameter (Density: 2000 kg/m^3)	Drag force, gravitational force	A small difference was found among particles with a diameter of 5 µm, 7 µm and 10 µm in terms of distribution and trajectory

Table 3 (continued)

Authors	Particles size	Forces	Findings
Mousavi and Grosskopf (2015)	1 µm in diameter	Drag force, gravitational force, Brownian force, Saffman's lift force, pressure gradient force	A combination of drag, gravitational, Brownian, pressure gradient, Saffman's lift forces are required to predict the particle trajectory in the hospital's anteroom and isolation room
King et al. (2013)	2.5 µm in diameter	Drag force, gravitational force, Saffman's lift force, Brownian force	The differences of particles distributions and flow trajectory are insignificant between 1 µm and 5 µm

(2015), Wu and Lin's (2015) technique is more practical in reflecting the naturalistic of human walking.

Meanwhile, Hang et al. (2014) and Tao et al. (2016) investigated the progression of movement by the simulation technique. They utilised the dynamic mesh and UDF codes to handle the moving effects. So far, there is still a discrepancy between the description of employing the dynamic mesh and the UDF. Also, verifying the selected airflow model to couple with the dynamic mesh required further attention. Table 4 summarised the methods used to investigate the motion effects in an indoor building.

Conclusion

The inadequate knowledge on the assessment of IAQ would retard the development of effective mitigations against airborne infectious diseases. Therefore, this paper presented a comprehensive review of the current methods to measure airflow and particle distribution in an indoor environment through experimental and numerical approaches. Studies have demonstrated that both the experimental and simulation methods are essential to evaluate the IAQ in healthcare facilities. The experimental works could provide valid, comprehensive, and actual data that reflects the in-situ condition. However, the results may only be applicable to a specific situation and become difficult to conduct parametric studies. In contrast, the simulation approaches can perform multiple case studies with a shorter turnaround time and lower cost. Therefore, the numerical approach has gained increasing attention and been widely utilised in relevant research. Nonetheless, verification of grid independence and validation of numerical models are essential to ensure the credibility and reliability of the simulated results. The selection of turbulence models, wall treatment function and the monitoring of residuals could pose significant impacts on the accuracy of the result. Though the numerical approach has been widely utilised by researchers, it could yet replace the experimental work, especially for the biological sampling of microbes. Furthermore, the exclusion of human movement in indoor airflow studies may lead to an underprediction of particle movement due to human-induced wake flow. In order to provide reliable and feasible engineering control measures for reducing the cross-infection of airborne infectious diseases in healthcare facilities, it is necessary to conduct in-depth research on the influence of movement and time-dependent studies, in particular on the transport of airborne infectious particles. As far as authors are concerned, the effects of various turning speeds and actual human walking movements such as foot stepping and arms swinging are limited. More comprehensive research in these areas could be the extended scopes which deserve to be explored.

Table 4 Summary of methods used in investigating the effects of movement in an indoor environment

Authors	Research area	Methods:	Findings
Wong et al. (2019b)	Operating room	Numerical simulation (CFD): Dynamic mrsh ~ Remeshing methods (Tetrahedral cells) Airflow model ~ RNG k-ε Algorithm ~ PISO	The bent-forearm and upright turnings of the manikin could increase the airflow velocity in the surgical zone by 35% and 23%, respectively
Hang et al. (2014)	Isolation room	Numerical simulation (CFD): Dynamic mesh ~ Not mention Airflow model ~ RNG k-ε Algorithm ~ SIMPLE	The human walking produced the flow disturbance and enhanced the airborne transmission from the source. The flow quantities including pressure, velocity, and turbulence near and behind human body are all easily influenced by the motion
Tao et al. (2016)	Controlled room	Numerical simulation (CFD): Dynamic mesh ~ Layering mesh method (Prism cells) Dimensional wall distance, $y^+ < 5$ Airflow model ~ RNG k-ε Algorithm ~ SIMPLE	Airflow momentum induced by the moving body disturbed the 2.5 µm particle that was initially at rest on the floor to lift and become re-suspended due to its interaction with the trailing wake
Wang and Chow (2015)	Isolation room	Numerical simulation (CFD): Dynamic mesh ~ Layering mesh method (Hexahedral cells) Airflow model ~ Standard k-ε Algorithm ~ SIMPLEC	The movement speed and posture significantly influenced the suspended droplets concentration in a room
Chang et al. (2016)	Control room	Numerical simulation (CFD): Dynamic mesh ~ Remeshing methods (Tetrahedral cells) Airflow model ~ RNG k-ε Algorithm ~ COUPLED	The leakage flow rate was always found to be positive. However, the leakage flow rate peaked at the beginning and end of the rotating period, and the flow rate was generally low during the direction-changing period
Mousavi and Grosskopf (2016)	Isolation room	Numerical simulation (CFD): Dynamic mesh ~ Layering and remeshing methods (Tetrahedral cells) Airflow model ~ Realisable k-ε	Higher door-opening speeds create turbulence and increase the rate of volume exchange under both negative and neutral pressure room conditions. Unidirectional airflow was disrupted during door opening motion
Shih et al. (2007)	Isolation room	Numerical simulation (CFD): Dynamic mesh Airflow model ~ k-ε Algorithm ~ SIMPLEC	The opening and closing of a sliding door affected the room internal pressure and velocity distributions. These movements have also induced the air from the anteroom flow into the isolation room
Kamar et al. (2020)	Operating room	Numerical simulation (CFD): Dynamic mesh Airflow model ~ RNG k-ε Algorithm ~ PISO	Replacing the turning bent-forearm medical staff with the stationary bent-forearm medical staff reduced the number of particles that settled on a patient by 60.9%, while substituting the turning straight-forearm medical staff with the stationary straight-forearm medical staff lowered the particle settlement by 37.5%
Wong et al. (2022)	Operating room	Numerical simulation (CFD): Dynamic mesh Airflow model ~ RNG k-ε Algorithm ~ PISO	The increment of ceiling-mounted air supply diffuser's area from 4.3 m^3 to 5.7 m^2 and 15.9 m^2 could reduce the particle settlement by 41% and 39%, respectively
Villafruela et al. (2016)	Operating room	Experimental (Onsite measurement of air velocity and air volume): Mechanical movement ~ Door opening and closing	An operating room which initially had an overpressure of 20 Pa is not capable of preventing the penetration of adjacent air during the opening of the sliding door
Kalliomäki et al. (2016)	Isolation room	Experimental (Smoke visualisation): Mechanical movement ~ Human manikin was fixed to a small cart moving along a rail running on the floor	Sliding door performed better than single hinged door under different ventilation setup. The air volume exchange across the doorway is relatively smaller when using the sliding door

Table 4 (continued)

Authors	Research area	Methods:	Findings
Kalliomäki et al. (2015)	Isolation room	Experimental (Smoke visualisation and tracer gas measurements): Mechanical movement ~ Human manikin was fixed to a small cart moving along a rail running on the floor	Based on smoke visualisation method, both sliding and hinged doors produced a detectable airflow through the doorway during the opening. The airflow changes; however, are more obvious for hinged door opening Based on the tracer gas measurement method, the air exchange volume was found to be significantly lower for the sliding door than for the hinged door
Wu and Lin (2015)	Waiting room	Experimental (Onsite measurement of velocity, temperature, and CO_2 concentration): Mechanical movement ~ Real human moving	The influence of human walking under the displacement ventilation is larger than the stratum and mixing ventilation. Stratum ventilation can keep relatively high ventilation efficiency when human movement is taken place
Teter et al. (2017)	Operating room	Experimental (Onsite measurement of particle count): Mechanical movement ~ Door opening and closing	The door opening increased the airborne particle counts of all sizes by 13%. Particles that larger than 0.5 μm in diameter elevated significantly when the door was opened
Wu et al. (2021)	Control room	Experimental (Onsite measurement of particle count): Human manikin was fixed to a wheelchair and a cart to move along a rail running on the floor	Manikin movement enhance the fuller mixing of indoor air and particles, as well as increase the particle suspension time
Bhattacharya et al. (2021)	Control room	Experimental (Onsite measurement of anemometer and particle count): Human manikin was fixed to move on a walking track	Walking on a straight line creates significant impacts in the velocity normal to the walking path, and vertical to the plane of walking movement, where the changes were detectable till 1.0 m away from the walking track

Author contribution All authors contributed to the study conception and design. Conceptualization, methodology and writing—original draft: Huiyi Tan; methodology, supervision, review and editing: Keng Yinn Wong; writing, review and editing: Mohd Hafiz Dzarfan Othman, Hong Yee Kek, Roswanira Abdul Wahab; resources, conceptualization: Garry Kuan Pei Ern; investigation, review and editing: Wen Tong Chong, Kee Quen Lee. All authors read and approved the final manuscript.

Funding This research was financially supported by the Mini Research Grant by the Institution of Mechanical Engineers (IMechE), Malaysia Branch and Universiti Teknologi Malaysia (UTM) Zamalah Grant, under the Vot No. 4C587 and 00N04, respectively.

Data availability Not applicable.

Declarations

Ethics approval and consent to participate Not applicable.

Consent for publication Not applicable.

Competing interests The authors declare no competing interests.

References

Adamu ZA, Price ADF, Cook MJ (2012) Performance evaluation of natural ventilation strategies for hospital wards —a case study of Great Ormond Street Hospital. Build Environ 56:211–222

Al-Waked R (2014) Effect of ventilation strategies on infection control inside operating theatres. Eng Appl Comput Fluid Mech 4:1–16

Allegranzi B, Bagheri Nejad S, Combescure C, Graafmans W, Attar H, Donaldson L, Pittet D (2011) Burden of endemic health-care-associated infection in developing countries: systematic review and meta-analysis. Lancet 377:228–241

ASHRAE (2013) ANSI/ASHRAE Standard 170–2013. American Society of Heating, Refrigerating and Air-Conditioning Engineers Inc, Atlanta

ASHRAE (2019) ASHRAE Handbook - HVAC Applications

Aubin J, Fletcher DF, Xuereb C (2004) Modeling turbulent flow in stirred tanks with CFD: the influence of the modeling approach, turbulence model and numerical scheme. Exp Thermal Fluid Sci 28:431–445

Azmir J, Hou Q, Yu A (2018) Discrete particle simulation of food grain drying in a fluidised bed. Powder Technol 323:238–249

Balocco C, Lio P (2011) Assessing ventilation system performance in isolation rooms. Energy Build 43:246–252

Balocco C, Petrone G, Cammarata G (2015) Numerical investigation of different airflow schemes in a real operating theatre. J Biomed Sci Eng 08:73–89

Barbadoro P, Bruschi R, Martini E, Savini S, Gioia M, Stoico R, Di Tondo E, D'Errico M, Prospero E (2016) Impact of laminar air flow on operating room contamination, and surgical wound infection rates in clean and contaminated surgery. Eur J Surg Oncol 42:1756–1758

Bhattacharya A, Pantelic J, Ghahramani A, Mousavi ES (2021) Three-dimensional analysis of the effect of human movement on indoor airflow patterns. Indoor Air 31:587–601

Birgand G, Toupet G, Rukly S, Antoniotti G, Deschamps M-N, Lepelletier D, Pornet C, Stern JB, Vandamme Y-M, van der Mee-Marquet N (2015) Air contamination for predicting wound contamination in clean surgery: A large multicenter study. Am J Infect Control 43:516–521

Bivolarova MP, Melikov AK, Mizutani C, Kajiwara K, Bolashikov ZD (2016) Bed-integrated local exhaust ventilation system combined with local air cleaning for improved IAQ in hospital patient rooms. Build Environ 100:10–18

Blomquist PH (2006) Methicillin-resistant Staphylococcus aureus infections of the eye and orbit (an American Ophthalmological Society thesis). Trans Am Ophthalmol Soc 104:322–345

Booth CM, Clayton M, Crook B, Gawn J (2013) Effectiveness of surgical masks against influenza bioaerosols. J Hosp Infect 84:22–26

Cabo Verde S, Almeida SM, Matos J, Guerreiro D, Meneses M, Faria T, Botelho D, Santos M, Viegas C (2015) Microbiological assessment of indoor air quality at different hospital sites. Res Microbiol 166:557–563

Calautit JK, Hughes BR (2014) Measurement and prediction of the indoor airflow in a room ventilated with a commercial wind tower. Energy Build 84:367–377

Cao G, Awbi H, Yao R, Fan Y, Sirén K, Kosonen R, Zhang J (2014) A review of the performance of different ventilation and airflow distribution systems in buildings. Build Environ 73:171–186

Chang L, Zhang X, Wang S, Gao J (2016) Control room contaminant inleakage produced by door opening and closing: dynamic simulation and experiments. Build Environ 98:11–20

Chao CYH, Wan MP, Morawska L, Johnson GR, Ristovski ZD, Hargreaves M, Mengersen K, Corbett S, Li Y, Xie X, Katoshevski D (2009) Characterization of expiration air jets and droplet size distributions immediately at the mouth opening. J Aerosol Sci 40:122–133

Chen C, Liu W, Li F, Lin C-H, Liu J, Pei J, Chen Q (2013) A hybrid model for investigating transient particle transport in enclosed environments. Build Environ 62:45–54

Chen CJ, Huang YC (2014) New epidemiology of Staphylococcus aureus infection in Asia. Clin Microbiol Infect 20:605–623

Chen F, Yu SCM, Lai ACK (2006) Modeling particle distribution and deposition in indoor environments with a new drift–flux model. Atmos Environ 40:357–367

Chen Y, Zhao JY, Shan X, Han XL, Tian SG, Chen FY, Su XT, Sun YS, Huang LY, Han L, Chinese Group on Point-Prevalence Survey of Healthcare-Associated I (2016) A point-prevalence survey of healthcare-associated infection in fifty-two Chinese hospitals. J Hosp Infect

Choi DH, Choi SH, Kang DH (2017) Influence of Surgical Smoke on Indoor Air Quality in Hospital Operating Rooms. Aerosol and Air Quality Research 17:821–830

Chow T-T, Wang J (2012) Dynamic simulation on impact of surgeon bending movement on bacteria-carrying particles distribution in operating theatre. Build Environ 57:68–80

Chow TT, Yang XY (2004) Ventilation performance in operating theatres against airborne infection: review of research activities and practical guidance. J Hosp Infect 56:85–92

Chow TT, Kwan A, Lin Z, Bai W (2006) Conversion of operating theatre from positive to negative pressure environment. J Hosp Infect 64:371–378

Clark RP, de Calcina-Goff ML (2009) Some aspects of the airborne transmission of infection. J R Soc Interface 6(Suppl 6):S767–S782

Cornelissen JT, Taghipour F, Escudié R, Ellis N, Grace JR (2007) CFD modelling of a liquid–solid fluidized bed. Chem Eng Sci 62:6334–6348

D'Alessandro D, Cerquetani F, Deriu MG, Montagna MT, Mura I, Napoli C, Vescia N (2013) Evaluation of fungal contamination in operating rooms using a dusting cloth pad: comparison among different sampling methods. Am J Infect Control 41:658–660

Dai C, Zhang Y, Ma X, Yin M, Zheng H, Gu X, Xie S, Jia H, Zhang L, Zhang W (2015) Real-time measurements of airborne biologic particles using fluorescent particle counter to evaluate microbial

contamination: results of a comparative study in an operating theater. Am J Infect Control 43:78–81
Davies A, Thomson G, Walker J, Bennett A (2009) A review of the risks and disease transmission associated with aerosol generating medical procedures. J Infect Prev 10:122–126
Duan R, Liu W, Xu L, Huang Y, Shen X, Lin C-H, Liu J, Chen Q, Sasanapuri B (2015) Mesh type and number for the CFD simulations of air distribution in an aircraft cabin. Numer Heat Transfer B Fundame 67:489–506
Faulkner WB, Memarzadeh F, Riskowski G, Kalbasi A, Ching-Zu Chang A (2015) Effects of air exchange rate, particle size and injection place on particle concentrations within a reduced-scale room. Build Environ 92:246–255
Ferziger JH, Peric M (2012) Computational methods for fluid dynamics. Springer Science & Business Media
Fluent A (2009) Ansys fluent 12.0 users guide, Ansys Inc. ANSYS, USA
Fontanesi S, Cicalese G, De Pasquale G (2015) A methodology for the reduction of numerical diffusion in sloshing analyses through automated mesh adaptation. Energy Procedia 81:856–865
Fu S, Biwole PH, Mathis C (2016) Numerical and experimental comparison of 3D particle tracking velocimetry (PTV) and particle image velocimetry (PIV) accuracy for indoor airflow study. Build Environ 100:40–49
Gilkeson CA, Noakes CJ, Khan MAI (2014) Computational fluid dynamics modelling and optimisation of an upper-room ultraviolet germicidal irradiation system in a naturally ventilated hospital ward. Indoor Built Environ 23:449–466
Guo ZD, Wang ZY, Zhang SF, Li X, Li L, Li C, Cui Y, Fu RB, Dong YZ, Chi XY, Zhang MY, Liu K, Cao C, Liu B, Zhang K, Gao YW, Lu B, Chen W (2020) Aerosol and surface distribution of severe acute respiratory syndrome coronavirus 2 in hospital wards, Wuhan, China, 2020. Emerg Infect Dis 26:1583–1591
Haig CW, Mackay WG, Walker JT, Williams C (2016) Bioaerosol sampling: sampling mechanisms, bioefficiency and field studies. J Hosp Infect 93:242–255
Hang J, Li Y, Jin R (2014) The influence of human walking on the flow and airborne transmission in a six-bed isolation room: Tracer gas simulation. Build Environ 77:119–134
Hang J, Li Y, Ching W, Wei J, Jin R, Liu L, Xie X (2015) Potential airborne transmission between two isolation cubicles through a shared anteroom. Build Environ 89:264–278
Hansen D, Krabs C, Benner D, Brauksiepe A, Popp W (2005) Laminar air flow provides high air quality in the operating field even during real operating conditions, but personal protection seems to be necessary in operations with tissue combustion. Int J Hyg Environ Health 208:455–460
Helmis CG, Tzoutzas J, Flocas HA, Halios CH, Stathopoulou OI, Assimakopoulos VD, Panis V, Apostolatou M, Sgouros G, Adam E (2007) Indoor air quality in a dentistry clinic. Sci Total Environ 377:349–365
Ho SH, Rosario L, Rahman MM (2009) Three-dimensional analysis for hospital operating room thermal comfort and contaminant removal. Appl Therm Eng 29:2080–2092
Hoffman PN, Williams J, Stacey A, Bennett AM, Ridgway GL, Dobson C, Fraser I, Humphreys H (2002) Microbiological commissioning and monitoring of operating theatre suites. J Hosp Infect 52:1–28
Hong S-W, Exadaktylos V, Lee I-B, Amon T, Youssef A, Norton T, Berckmans D (2017) Validation of an open source CFD code to simulate natural ventilation for agricultural buildings. Comput Electron Agric 138:80–91
Horve PF, Dietz LG, Fretz M, Constant DA, Wilkes A, Townes JM, Martindale RG, Messer WB, Van Den Wymelenberg KG (2021) Identification of SARS-CoV-2 RNA in healthcare heating, ventilation, and air conditioning units. Indoor Air 31:1826–1832
Huang Y, Pei J, V. Nielsen P, Bonthoux F, Lechene S, Keller F-x, Wu S, Xu C, Cao Z (2021) Chapter 4 - Experimental techniques. In: Goodfellow HD , Wang Y (Editors), Industrial Ventilation Design Guidebook (Second Edition). Academic Press, pp. 185-277
Hubad B, Lapanje A (2012) Inadequate hospital ventilation system increases the risk of nosocomial Mycobacterium tuberculosis. J Hosp Infect 80:88–91
Hurnik M, Blaszczok M, Popiolek Z (2015) Air distribution measurement in a room with a sidewall jet: A 3D benchmark test for CFD validation. Build Environ 93:319–330
Jin X, Yang L, Du X, Yang Y (2015) Particle transport characteristics in indoor environment with an air cleaner. Indoor Built Environ 25:987–996
Jin X, Yang L, Du X, Yang Y (2016) Particle transport characteristics in indoor environment with an air cleaner. Indoor Built Environ 25:987–996
Jurelionis A, Gagytė L, Prasauskas T, Čiužas D, Krugly E, Šeduikytė L, Martuzevičius D (2015) The impact of the air distribution method in ventilated rooms on the aerosol particle dispersion and removal: The experimental approach. Energy Build 86:305–313
Kalliomäki P, Saarinen P, Tang JW, Koskela H (2015) Airflow patterns through single hinged and sliding doors in hospital isolation rooms. Int J Vent 14:111–126
Kalliomäki P, Saarinen P, Tang JW, Koskela H (2016) Airflow patterns through single hinged and sliding doors in hospital isolation rooms–Effect of ventilation, flow differential and passage. Build Environ 107:154–168
Kamar HM, Wong KY, Kamsah N (2020) The effects of medical staff turning movements on airflow distribution and particle concentration in an operating room. J Build Perform Simul 13:684–706
Kamsah N, Kamar HM, Alhamid MI, Wong KY (2018) Impacts of temperature on airborne particles in a hospital operating room. J Adv Res Fluid Mech Thermal Sci 44:12–23
Karimi M, Akdogan G, Dellimore KH, Bradshaw SM (2012) Quantification of numerical uncertainty in computational fluid dynamics modelling of hydrocyclones. Comput Chem Eng 43:45–54
Khankari K (2016) Patient Room HVAC. ASHRAE J 58:16
Kim SH, Augenbroe G (2013) Decision support for choosing ventilation operation strategy in hospital isolation rooms: a multi-criterion assessment under uncertainty. Build Environ 60:305–318
King M-F, Noakes C, Sleigh P, Camargo-Valero M (2013) Bioaerosol deposition in single and two-bed hospital rooms: a numerical and experimental study. Build Environ 59:436–447
Krambrich J, Akaberi D, Ling J, Hoffman T, Svensson L, Hagbom M, Lundkvist A (2021) SARS-CoV-2 in hospital indoor environments is predominantly non-infectious. Virol J 18:109
Kuznik F, Rusaouën G, Brau J (2007) Experimental and numerical study of a full scale ventilated enclosure: comparison of four two equations closure turbulence models. Build Environ 42:1043–1053
Kwaśniewski L (2013) Application of grid convergence index in FE computation. Bull Polish Acad Sci Tech Sci 61:123–128
Lapid-Gortzak R, Traversari R, Linden JW, Oberstein SYL, Lapid O, Schlingemann RO (2016) Mobile ultra-clean unidirectional airflow screen reduces air contamination in a simulated setting for intra-vitreal injection. Int Ophthalmol 1–7
Layden JE, Ghinai I, Pray I, Kimball A, Layer M, Tenforde MW, Navon L, Hoots B, Salvatore PP, Elderbrook M, Haupt T, Kanne J, Patel MT, Saathoff-Huber L, King BA, Schier JG, Mikosz CA, Meiman J (2020) SARS-CoV-2 viral load in upper respiratory specimen of infected patients. N Engl J Med 382:903–916
Lee S, Park B, Kurabuchi T (2016) Numerical evaluation of influence of door opening on interzonal air exchange. Build Environ 102:230–242

Lewis BD, Spencer M, Rossi PJ, Lee CJ, Brown KR, Malinowski M, Seabrook GR, Edmiston CE Jr (2015) Assessment of an innovative antimicrobial surface disinfectant in the operating room environment using adenosine triphosphate bioluminescence assay. Am J Infect Control 43:283–285

Li A, Gou L, Wang X, Zhang Y (2016a) 2D-PIV experiment analysis on the airflow performance of a floor-based air distribution with a novel mushroom diffuser (FBAD-MD). Energy Build 121:114–129

Li F, Lee ES, Liu J, Zhu Y (2015a) Predicting self-pollution inside school buses using a CFD and multi-zone coupled model. Atmos Environ 107:16–23

Li F, Liu J, Ren J, Cao X, Zhu Y (2016b) Numerical investigation of airborne contaminant transport under different vortex structures in the aircraft cabin. Int J Heat Mass Transf 96:287–295

Li H, Zou ZJ, Wang F (2014) The effect of air change rate and cleanroom garment on cleanliness in grade B cleanroom, Applied Mechanics and Materials. Trans Tech Publ 514–517

Li J, Cao X, Liu J, Wang C, Zhang Y (2015b) Global airflow field distribution in a cabin mock-up measured via large-scale 2D-PIV. Building and Environment 93. Part 2:234–244

Li X, Yan Y, Tu J (2015c) The simplification of computer simulated persons (CSPs) in CFD models of occupied indoor spaces. Building and Environment 93. Part 2:155–164

Liang C-C, Wu F-J, Chien T-Y, Lee S-T, Chen C-T, Wang C, Wan G-H (2020) Effect of ventilation rate on the optimal air quality of trauma and colorectal operating rooms. Build Environ 169

Lin CH, Wu TT, Horstman RH, Lebbin PA, Hosni MH, Jones BW, Beck BT (2006) Comparison of large Eddy Simulation predictions with particle image velocimetry data for the airflow in a generic cabin model. HVAC&R Research 12:935–951

Link T, Kleiner C, Mancuso MP, Dziadkowiec O, Halverson-Carpenter K (2016) Determining high touch areas in the operating room with levels of contamination. American journal of infection control

Liu C, Zhou G, Li H (2015) Analysis of thermal environment in a hospital operating room. Procedia Eng 121:735–742

Liu J, Wang H, Wen W (2009) Numerical simulation on a horizontal airflow for airborne particles control in hospital operating room. Build Environ 44:2284–2289

Lu W, Howarth AT, Adam N, Riffat SB (1996) Modelling and measurement of airflow and aerosol particle distribution in a ventilated two-zone chamber. Build Environ 31:417–423

Lu Y, Oladokun M, Lin Z (2020) Reducing the exposure risk in hospital wards by applying stratum ventilation system. Build Environ 183

Mahyuddin N, Awbi HB, Essah EA (2015) Computational fluid dynamics modelling of the air movement in an environmental test chamber with a respiring manikin. J Build Perform Simul 8:359–374

Månsson E, Hellmark B, Sundqvist M, Söderquist B (2015) Sequence types of Staphylococcus epidermidis associated with prosthetic joint infections are not present in the laminar airflow during prosthetic joint surgery. APMIS 123:589–595

Memarzadeh F, Manning A (2003) Reducing risks of surgery. ASHRAE Journal February, 28–33

Méndez C, San José JF, Villafruela JM, Castro F (2008) Optimization of a hospital room by means of CFD for more efficient ventilation. Energy Build 40:849–854

Milton DK, Fabian MP, Cowling BJ, Grantham ML, McDevitt JJ (2013) Influenza virus aerosols in human exhaled breath: particle size, culturability, and effect of surgical masks. PLoS Pathog 9:e1003205

Morawska L, Johnson GR, Ristovski ZD, Hargreaves M, Mengersen K, Corbett S, Chao CYH, Li Y, Katoshevski D (2009) Size distribution and sites of origin of droplets expelled from the human respiratory tract during expiratory activities. J Aerosol Sci 40:256–269

Mousavi ES, Grosskopf KR (2015) Directional airflow and ventilation in hospitals: a case study of secondary airborne infection. Energy Procedia 78:1201–1206

Mousavi ES, Grosskopf KR (2016) Airflow patterns due to door motion and pressurization in hospital isolation rooms. Sci Technol Built Environ 1–6

Muller MP, MacDougall C, Lim M, Armstrong I, Bialachowski A, Callery S, Ciccotelli W, Cividino M, Dennis J, Hota S, Garber G, Johnstone J, Katz K, McGeer A, Nankoosingh V, Richard C, Vearncombe M (2016) Antimicrobial surfaces to prevent healthcare-associated infections: a systematic review. J Hosp Infect 92:7–13

Nastase I, Croitoru C, Vartires A, Tataranu L (2016) Indoor environmental quality in operating rooms: an European standards review with regard to Romanian guidelines. Energy Procedia 85:375–382

Nielsen PV (2015) Fifty years of CFD for room air distribution. Build Environ 91:78–90

Nimlyat PS, Kandar MZ (2015) Appraisal of indoor environmental quality (IEQ) in healthcare facilities: A literature review. Sustain Cities Soc 17:61–68

Noguchi C, Koseki H, Horiuchi H, Yonekura A, Tomita M, Higuchi T, Sunagawa S, Osaki M (2017) Factors contributing to airborne particle dispersal in the operating room. BMC Surg 17:78

Olmsted RN (2008) Pilot study of directional airflow and containment of airborne particles in the size of Mycobacterium tuberculosis in an operating room. Am J Infect Control 36:260–267

Otter JA, Donskey C, Yezli S, Douthwaite S, Goldenberg SD, Weber DJ (2016) Transmission of SARS and MERS coronaviruses and influenza virus in healthcare settings: the possible role of dry surface contamination. J Hosp Infect 92:235–250

Pankhurst L, Taylor J, Cloutman-Green E, Hartley J, Lai K (2011) Can clean-room particle counters be used as an infection control tool in hospital operating theatres? Indoor Built Environ 1420326X11409467

Park J-Y, Sung M (2015) A study on the contaminant dispersion from isolation ward under abnormal operation of facilities. Energy Procedia 78:1239–1244

Peng L, Nielsen PV, Wang X, Sadrizadeh S, Liu L, Li Y (2016) Possible user-dependent CFD predictions of transitional flow in building ventilation. Build Environ 99:130–141

Pletcher RH, Tannehill JC, Anderson D (2012) Computational fluid mechanics and heat transfer. CRC Press

Poussou SB, Mazumdar S, Plesniak MW, Sojka PE, Chen Q (2010) Flow and contaminant transport in an airliner cabin induced by a moving body: model experiments and CFD predictions. Atmos Environ 44:2830–2839

Prevention CDC (2007) S. aureus and MRSA surveillance summary 2007. Department of Health and Human Services, Centres for Disease Control and Prevention October 17

Prevention CDC (2017) Guidelines for environmental infection control in health-care facilities, US Department of Health and Human Services. Centers for Disease Control and Prevention

Qian H, Li Y, Nielsen PV, Hyldgaard CE (2008) Dispersion of exhalation pollutants in a two-bed hospital ward with a downward ventilation system. Build Environ 43:344–354

Rai AC, Lin C-H, Chen Q (2014) Numerical modeling of volatile organic compound emissions from ozone reactions with human-worn clothing in an aircraft cabin. HVAC&R Res 20:922–931

Reyes VA, Sierra-Espinosa FZ, Moya SL, Carrillo F (2015) Flow field obtained by PIV technique for a scaled building-wind tower model in a wind tunnel. Energy Build 107:424–433

Roache PJ (1993) A method for uniform reporting of grid refinement studies. ASME-PUBLICATIONS-FED 158:109–109

Roache PJ (1998) Verification and validation in computational science and engineering, 895. Hermosa Albuquerque, NM

Romano F, Marocco L, Gustén J, Joppolo CM (2015) Numerical and experimental analysis of airborne particles control in an operating theater. Build Environ 89:369–379

Romano F, Gustén J, De Antonellis S, Joppolo C (2017) Electrosurgical smoke: ultrafine particle measurements and work environment quality in different operating theatres. Int J Environ Res Public Health 14:137

Ryan-Fogarty Y, O'Regan B, Moles R (2016) Greening healthcare: systematic implementation of environmental programmes in a university teaching hospital. J Clean Prod 126:248–259

Sadrizadeh S, Holmberg S (2014) Surgical clothing systems in laminar airflow operating room: a numerical assessment. J Infect Public Health 7:508–516

Sadrizadeh S, Holmberg S, Tammelin A (2014a) A numerical investigation of vertical and horizontal laminar airflow ventilation in an operating room. Build Environ 82:517–525

Sadrizadeh S, Tammelin A, Ekolind P, Holmberg S (2014b) Influence of staff number and internal constellation on surgical site infection in an operating room. Particuology 13:42–51

Sadrizadeh S, Holmberg S (2015) Effect of a portable ultra-clean exponential airflow unit on the particle distribution in an operating room. Particuology 18:170–178

Sadrizadeh S, Afshari A, Karimipanah T, Håkansson U, Nielsen PV (2016a) Numerical simulation of the impact of surgeon posture on airborne particle distribution in a turbulent mixing operating theatre. Build Environ 110:140–147

Sadrizadeh S, Holmberg S, Nielsen PV (2016b) Three distinct surgical clothing systems in a turbulent mixing operating room equipped with mobile ultraclean laminar airflow screen: A numerical evaluation. Sci Technol Built Environ 22:337–345

Sadrizadeh S, et al. (2021) A systematic review of operating room ventilation. J Build Eng 40

Saito Y, Yasuhara H, Murakoshi S, Komatsu T, Fukatsu K, Uetera Y (2015) Time-dependent influence on assessment of contaminated environmental surfaces in operating rooms. Am J Infect Control 43:951–955

Salim SM, Viswanathan S, Ray MB (2006) Evaluation of source model coupled computational fluid dynamics (CFD) simulation of the dispersion of airborne contaminants in a work environment. J Occup Environ Hyg 3:684–693

Sanzen L, Carlsson AS, Walder M (1989) Occlusive clothing and ultraviolet radiation in hip surgery. Acta Orthop Scand 60:664–667

Satheesan MK, Mui KW, Wong LT (2020) A numerical study of ventilation strategies for infection risk mitigation in general inpatient wards. Build Simul 1–10

Saw LH, Leo BF, Nor NSM, Yip CW, Ibrahim N, Hamid HHA, Latif MT, Lin CY, Nadzir MSM (2021) Modeling aerosol transmission of SARS-CoV-2 from human-exhaled particles in a hospital ward. Environ Sci Pollut Res Int 28:53478–53492

Shaw LF, Chen CS, Wu HH, Lai LS, Chen YY, Wang FD (2018) Factors influencing microbial colonies in the air of operating rooms. BMC Infect Dis 18:4

Shih Y-C, Chiu C-C, Wang O (2007) Dynamic airflow simulation within an isolation room. Build Environ 42:3194–3209

Srebric J, Chen Q (2002) Simplified numerical models for complex air supply diffusers. HVAC&R Res 8:277–294

Srivastava S, Zhao X, Manay A, Chen Q (2021) Effective ventilation and air disinfection system for reducing coronavirus disease 2019 (COVID-19) infection risk in office buildings. Sustain Cities Soc 75:103408

Swan JS, Deasy EC, Boyle MA, Russell RJ, O'Donnell MJ, Coleman DC (2016) Elimination of biofilm and microbial contamination reservoirs in hospital washbasin U-bends by automated cleaning and disinfection with electrochemically activated solutions. J Hosp Infect 94:169–174

Tan H, Wong KY, Dzarfan Othman MH, Kek HY, Tey WY, Nyakuma BB, Mong GR, Kuan G, Ho WS, Kang HS, Chin Vui Sheng DD, Wahab RA (2022a) Controlling infectious airborne particle dispersion during surgical procedures: why mobile air supply units matter? Build Environ 223:109489

Tan H, Wong KY, Lee CT, Wong SL, Nyakuma BB, Wahab RA, Lee KQ, Chiong MC, Ho WS, Othman MHD, Kek HY, Yau YH, Kamar HM (2022b) Numerical assessment of ceiling-mounted air curtain on the particle distribution in surgical zone. Journal of Thermal Analysis and Calorimetry

Tan H, Wong KY, Nyakuma BB, Kamar HM, Chong WT, Wong SL, Kang HS (2022c) Systematic study on the relationship between particulate matter and microbial counts in hospital operating rooms. Environ Sci Pollut Res Int 29:6710–6721

Tang JW, Eames I, Li Y, Taha YA, Wilson P, Bellingan G, Ward KN, Breuer J (2005) Door-opening motion can potentially lead to a transient breakdown in negative-pressure isolation conditions: the importance of vorticity and buoyancy airflows. J Hosp Infect 61:283–286

Tao Y, Inthavong K, Tu J (2016) Computational fluid dynamics study of human-induced wake and particle dispersion in indoor environment. Indoor Built Environ 1420326X16661025

Tao Y, Inthavong K, Petersen P, Mohanarangam K, Yang W, Tu J (2018) Experimental visualisation of wake flows induced by different shaped moving manikins. Build Environ 142:361–370

Teter J, Guajardo I, Al-Rammah T, Rosson G, Perl TM, Manahan M (2017) Assessment of operating room airflow using air particle counts and direct observation of door openings. Am J Infect Control 45:477–482

Toja-Silva F, Peralta C, Lopez-Garcia O, Navarro J, Cruz I (2015) Roof region dependent wind potential assessment with different RANS turbulence models. J Wind Eng Ind Aerodyn 142:258–271

Ufat H, Kaynakli O, Yamankaradeniz N, Yamankaradeniz R (2017) Three-dimensional air distribution analysis of different outflow typed operating rooms at different inlet velocities and room temperatures. Adv Mech Eng 9:1687814017707414

Vardoulakis S, Giagloglou E, Steinle S, Davis A, Sleeuwenhoek A, Galea KS, Dixon K, Crawford JO (2020) Indoor exposure to selected air pollutants in the home environment: a systematic review. Int J Environ Res Public Health 17

Verma TN, Sahu AK, Sinha SL (2017) Study of particle dispersion on one bed hospital using computational fluid dynamics. Mater Today Proceedings 4:10074–10079

Villafruela J, San José J, Castro F, Zarzuelo A (2016) Airflow patterns through a sliding door during opening and foot traffic in operating rooms. Build Environ 109:190–198

Villafruela JM, Castro F, San José JF, Saint-Martin J (2013) Comparison of air change efficiency, contaminant removal effectiveness and infection risk as IAQ indices in isolation rooms. Energy Build 57:210–219

Villafruela JM, Olmedo I, Berlanga FA, de Adana MR (2019) Assessment of displacement ventilation systems in airborne infection risk in hospital rooms. PLoS ONE 14:e0211390

Volk A, Ghia U, Stoltz C (2017) Effect of grid type and refinement method on CFD-DEM solution trend with grid size. Powder Technol 311:137–146

Wagner JA, Schreiber KJ (2014) Improving operating room contamination control. ASHRAE J 56:18

Wang H, Qian H, Zhou R, Zheng X (2020) A novel circulated air curtain system to confine the transmission of exhaled contaminants: A numerical and experimental investigation. Build Simul 1–13

Wang J, Chow T-T (2011) Numerical investigation of influence of human walking on dispersion and deposition of expiratory droplets in airborne infection isolation room. Build Environ 46:1993–2002

Wang J, Chow T-T (2015) Influence of human movement on the transport of airborne infectious particles in hospital. J Build Perform Simul 8:205–215

Wang M, Lin C-H, Chen Q (2012) Advanced turbulence models for predicting particle transport in enclosed environments. Build Environ 47:40–49

Weber DJ, Hoffmann KK, Rutala WA, Pyatt DG (2009) Control of healthcare-associated Staphylococcus aureus survey of practices in North Carolina Hospitals. Infect Control Hosp Epidemiol 30:909–911

Wendlandt R, Thomas M, Kienast B, Schulz AP (2016) In-vitro evaluation of surgical helmet systems for protecting surgeons from droplets generated during orthopaedic procedures. J Hosp Infect 94:75–79

Wong K, Kamar H, Kamsah N (2019a) Enhancement of airborne particles removal in a hospital operating room. Int J Automot Mech Eng 16:7447–7463

Wong KY, Haslinda MK, Nazri K, Alia SN (2019b) Effects of surgical staff turning motion on airflow distribution inside a hospital operating room. Evergreen 6:52–58

Wong KY, Tan H, Nyakuma BB, Kamar HM, Tey WY, Hashim H, Chiong MC, Wong SL, Wahab RA, Mong GR, Ho WS, Othman MHD, Kuan G (2022) Effects of medical staff's turning movement on dispersion of airborne particles under large air supply diffuser during operative surgeries. Environ Sci Pollut Res

Woods J, Braymen D, Rasmussen R, Reynolds G, Montag G (1986) Ventilation requirements in hospital operating rooms. I: Control of airborne particles. ASHRAE Trans 92:396–426

Wu J, Weng W, Shen L, Fu M (2021) Transient and continuous effects of indoor human movement on nanoparticle concentrations in a sitting person's breathing zone. Sci Total Environ 805:149970

Wu W, Lin Z (2015) An experimental study of the influence of a walking occupant on three air distribution methods. Build Environ 85:211–219

Xu C, Nielsen PV, Liu L, Jensen RL, Gong G (2017) Human exhalation characterization with the aid of schlieren imaging technique. Build Environ 112:190–199

Yan Y, Li X, Tu J (2016a) Effects of passenger thermal plume on the transport and distribution characteristics of airborne particles in an airliner cabin section. Sci Technol Built Environ 22:153–163

Yan Y, Li X, Yang L, Tu J (2016b) Evaluation of manikin simplification methods for CFD simulations in occupied indoor environments. Energy Build 127:611–626

Yau Y, Ding L (2014) A case study on the air distribution in an operating room at Sarawak General Hospital Heart Centre (SGHHC) in Malaysia. Indoor Built Environ 23:1129–1141

Yau YH, Chandrasegaran D, Badarudin A (2011) The ventilation of multiple-bed hospital wards in the tropics: a review. Build Environ 46:1125–1132

Yin H, Li A, Liu Z, Sun Y, Chen T (2016) Experimental study on airflow characteristics of a square column attached ventilation mode. Build Environ 109:112–120

Yin Y, Gupta JK, Zhang X, Liu J, Chen Q (2011) Distributions of respiratory contaminants from a patient with different postures and exhaling modes in a single-bed inpatient room. Build Environ 46:75–81

You R, Chen J, Shi Z, Liu W, Lin C-H, Wei D, Chen Q (2016a) Experimental and numerical study of airflow distribution in an aircraft cabin mock-up with a gasper on. J Build Perform Simul 9:555–566

You R, Liu W, Chen J, Lin C-H, Wei D, Chen Q (2016b) Predicting airflow distribution and contaminant transport in aircraft cabins with a simplified gasper model. J Build Perform Simul 9:699–708

You R, Chen J, Lin C-H, Wei D, Chen Q (2017) Investigating the impact of gaspers on cabin air quality in commercial airliners with a hybrid turbulence model. Build Environ 111:110–122

Young SW, Zhu M, Shirley OC, Wu Q, Spangehl MJ (2016) Do "surgical helmet systems" or "body exhaust suits" affect contamination and deep infection rates in arthroplasty? A Systematic Review. J Arthroplasty 31:225–233

Yu HC, Mui KW, Wong LT, Chu HS (2017) Ventilation of general hospital wards for mitigating infection risks of three kinds of viruses including Middle East respiratory syndrome coronavirus. Indoor Built Environ 26:514–527

Zhang H, Li D, Xie L, Xiao Y (2015) Documentary research of human respiratory droplet characteristics. Procedia Eng 121:1365–1374

Zhang L, Li Y (2012) Dispersion of coughed droplets in a fully-occupied high-speed rail cabin. Build Environ 47:58–66

Zhang Z, Chen Q (2007) Comparison of the Eulerian and Lagrangian methods for predicting particle transport in enclosed spaces. Atmos Environ 41:5236–5248

Zhang Z, Chen X, Mazumdar S, Zhang T, Chen Q (2009) Experimental and numerical investigation of airflow and contaminant transport in an airliner cabin mockup. Build Environ 44:85–94

Zhong L, Yuan J, Fleck B (2019) Indoor environmental quality evaluation of lecture classrooms in an institutional building in a cold climate. Sustainability 11

Zhou Q, Qian H, Liu L (2018) Numerical investigation of airborne infection in naturally ventilated hospital wards with central-corridor type. Indoor Built Environ 27:59–69

Zhu S, Srebric J, Spengler JD, Demokritou P (2012) An advanced numerical model for the assessment of airborne transmission of influenza in bus microenvironments. Build Environ 47:67–75

Publisher's note Springer Nature remains neutral with regard to jurisdictional claims in published maps and institutional affiliations.

Springer Nature or its licensor holds exclusive rights to this article under a publishing agreement with the author(s) or other rightsholder(s); author self-archiving of the accepted manuscript version of this article is solely governed by the terms of such publishing agreement and applicable law.